Chapter 2:

Laser Irradiation Effect on Optical Properties of Chalcogenide Glasses

Optical absorption measurements are widely used for studying disorder and defects in a-semiconductors. Optical absorption measurements are also very useful for studying the modifications of the density of states upon alloying and laser irradiating. The disorder and the defects have a strong influence on the band structure of Chalcogenide Glasses (ChGs) and the detailed electronic structure of a given Chalcogenide glass (ChG) are determined by the chemical bonding which occurs and therefore by its composition. Recently, there has been an increasing interest in semiconductor thin films due to their exceptional properties, which are remarkably different from those of bulk materials. ChGs are well-known and promising materials for a variety of photonic applications. The interest in these materials stems principally due to low phonon energy, extended infrared transparency, high refractive index, high photosensitivity, in reversible phase change optical recording etc [1-3]. Se-Te based alloys have created extreme interest due to their greater hardness, higher photosensitivity, higher crystallization temperature, and lower aging effects as in comparison to pure amorphous Se [4, 5]. It has been pointed out that Se-Te based alloys have more advantages than a-Se from the technological point of view. Addition of Te into Se improves the corrosion resistance [6]. Therefore, Se-Te based alloys are thought to be promising media, which make use of, a phase change between an amorphous state and a crystalline state and used to extend the utility of a-Se. Selenium–Tellurium based semiconductors have been the focus of interest in thin film form because of properties suitable for device applications [7, 8]. These glasses are optically highly non-linear and sensitive to the absorption of electromagnetic radiation and show a variety of photo-induced effects pursuant to illumination. Se–Te form a continuous series of solid solutions [9] and the Se–Te system has an intermediate behaviour between pure Se and pure Te. The addition of Te has a catalytic effect on the crystallization of Se. The presence of Te in Se chains probably favours thermal dissociation, the Se–Te bond being weaker than the Se–Se bond. This makes crystallization easier, by facilitating the close packing of a few Se chains to form a nucleation centre. An enhanced interaction between chains when Te is introduced is probably also conducive to crystallization. In the Se–Te alloy series, it is interesting to investigate the gradual change of the strange behaviour of Se to the normal behaviour. The important differences between elements exist in the character of band gap. In contrast to Te [10], the smaller gap of Se is an indirect one [11] so that in the Se–Te system a transition from the direct band gap of Te to the indirect band gap of Se must occur. The

ISBN: 978-81-936820-2-9
Thesis DOI: 10.21467/thesis.2

investigation of these properties with laser irradiation thus provides an understanding of the mechanism of degradation in these materials.

Exposure to light or other radiations like laser that excites electron-hole pair produces structural changes in nearly all ChGs and amorphous films. This causes a change in atomic configuration and a subsequent change in the physical and chemical properties such as structure, optical and electronic transport properties of the material [12-22]. The absorption of laser irradiation in chalcogenide thin film depends strongly on their electronic structure which in turn changes by the interaction with photons. The additional absorption of Te containing glasses is due to the increase in the number of thermally excited free carriers with Te content. The most important applications of chalcogenide are now in the field of optics [23-28] and arising mainly from either their exhibited infrared transmitting properties or photo-induced effects [29, 30]. Their potential uses have been reported [31-35] in integrated optics, optical imaging, optical data storage and infrared optics. Se-Te based alloys have gained much attention and found to be useful in practical application [36]. Among various applications of these chalcogenides, the optical recording of information has a leading importance. The principle underlying optical recording consists in the appearance of large change of certain physical and chemical parameters of the chalcogenides under the action of light. The energy of the light quanta situated in the UV spectral range is expected to induce qualitatively new changes in the ChGs, because this energy is equal or higher than the chemical bond energy.

The aim of the present work is to prepare amorphous Se-Te based glassy alloy with different additive by melt quenching technique and to investigate the laser irradiation effect on optical properties of prepared glassy alloys. To investigate the effect of laser irradiation on optical properties of prepared glassy alloys, thin films of each composition have been prepared by thermal evaporation technique. Prepared amorphous thin films have been irradiated with a pulsed Transverse Electrical Excitation at Atmospheric pressure (TEA) Nitrogen Laser and characterized before and after different time of irradiation by using UV/Visible Spectrophotometer.

2.1 Optical Properties of a-Semiconductors

The effect of disorder in the electronic structure of a-semiconductors is the redistribution of the states at the band edges in creation of tails of localized states which extend into the gap. Hence, unlike a crystalline semiconductor, the band edges are not discontinuous feature. These band tails originate from the distortions of the bond length and angle. Another feature of electronic structure of a-semiconductor is the presence of electronic states deep within the band gap which arise from the defects present in system such as coordination defects. Due to the absence of periodicity the momentum conservation rules for direct and indirect optical transitions are no longer applied. It is suggested that the optical transitions in a-semiconductors to be described by indirect transition model in which conservation of energy

and not the wave vector is significant [37]. In a-semiconductors, the optical absorption associated with the band to band transition is given by the product of joint density of states of conduction and valence band with transition probability [38]

In c-semiconductors, translational periodicity only permits excitations in which the wave vectors of initial and final states are conserved whereas in a-semiconductors this restriction does not apply [39]. In a-semiconductors, due to the presence of band tails and a wide distribution of defect states in the gap, the absorption coefficient does not show any sharp drop at any energy which would correspond to the band edge separation. An "optical band gap" (E_g) is usually defined by extrapolation of the observed absorption coefficient behavior in the high energy range where the absorption can be assigned to transitions between extended states in both bands. In addition, it is not yet clear whether the obtained energy gap represents band gap or mobility gap or something in between. At energies smaller than the optical band gap, the residual optical absorption is due to transitions involving localized states in the pseudo-gap as initial or/and final states and can therefore provide information on disorder and defects [40].

Analysis of optical absorption spectra provides essential information about band structure in both crystalline and non-crystalline materials. Optical absorption measurements are widely used for studying disorder and defects in a-semiconductors. Optical absorption measurements are also very useful for studying the modifications of the density of states upon alloying. Measurement of the absorption coefficient (α) as a function of frequency (ν) provides a mean to determine the optical band gap (E_g) of thin film. The absorption coefficient has been calculated directly from the following well known relation [41, 42]-

$$\alpha = \frac{1}{t}\ln\left(I/I_0\right) \qquad (2.1)$$

where "t" is the film thickness and $\ln\left(I/I_0\right)$corresponds to absorbance, neglecting the reflection coefficient, which is negligible and insignificant near the absorption edge.

The disorder and the defects have a strong influence on the band structure of ChGs and the fundamental optical absorption edge is one of the most sensitive methods for studying the electronic structure of both crystalline and a-semiconductors. The optical absorption edge in a-semiconductors is generally not as steep as that in crystalline semiconductors. In general, the absorption coefficient α can be divided into three parts [37, 43-45]:

(I) For $\alpha \leq 10^0$ cm^{-1}, a weak absorption tail exists with the form of-

$$\alpha \propto exp\left(\frac{h\nu}{E_w}\right) \qquad (2.2)$$

In this case the absorption spectrum describes optical transitions from the localized states attributed to the dangling bond defects to the extended states in the conduction band [46, 47].

(I) Urbach [48] reported that for $10^4 \geq \alpha \geq 10^0$ cm^{-1} the Urbach edge appears near the band edge and shows an exponential dependence on photon energy ($h\nu$)with the form of-

$$\alpha \propto exp\left(\frac{h\nu}{E_U}\right) \quad (2.3)$$

where E_U is the width of the band tail of the localized states in the band gap, also known as Urbach energy. The optical absorption for low values of α is mainly attributed to the transitions from the localized valence band tail states with an exponentially decreasing density of states function towards extended states in the conduction band. The width of the localized states depends on the degree of disorder and defects present in the amorphous structure. Magnitude of E_U has been calculated by taking slope of $\ln \alpha$ versus $h\nu$ curve.

(II) In the high absorption region for $\alpha \geq 10^4$ cm^{-1} optical absorption is attributed to the transitions from the extended states in the valence band to the extended states in the conduction band and the spectrum shows a square root dependence with photon energy ($h\nu$) given by Tauc et al [49] and discussed in more general terms by Devis and Mott [50, 51], whose equation is in the form of-

$$\alpha h\nu = \beta\left(h\nu - E_g\right)^n \quad (2.4)$$

where β is a constant, E_g is the optical energy gap of the material. The phonon absorption in many amorphous materials is found to obey the Tauc's relation. The index n is a number which characterizes the transition process involved. n has discrete values like 1/2, 3/2, 2 or more depending on whether the transition is direct or indirect and allowed or forbidden, respectively. In the direct and allowed cases, the index n is 1/2 whereas for the direct but forbidden cases it is 3/2. But for the indirect and allowed cases n=2 and for the forbidden cases it will be 3 or more. According to Tauc [52] the absorption tail related to localized states into the pseudo-gap, which localized states can arise from the existence of vacancy defects and/or impurities. The optical band gap(E_g) have been measured from the plot $(\alpha h\nu)^{1/2}$versus $h\nu$ by extrapolating the curves to $h\nu$ axis at $(\alpha h\nu)^{1/2} = 0$

2.2 Experimental Procedure

Optical study and effect of laser irradiation on optical properties has been carried out on different chalcogenide alloys. First the melt-quenching technique has been adopted to prepare all compositions of the investigated glassy systems. The procedure is described in next section. The as-quenched glassy alloys have been grounded and the resulting fine powder has been used to prepare the thin films by physical vapor deposition (PVD) method on properly cleaned glass slides. The prepared films have been characterized by using XRD. The optical absorbance (*A*) and transmittance (*T*) were recorded using Camspec model M550

UV/VIS/NIR double beam spectrometer in the wavelength range 190 –1100 nm. Laser irradiation has been carried out using pulsed Transverse Electrical Excitation at Atmospheric pressure (TEA) Nitrogen laser (wavelength 337.1 nm, peak power 100 kW, and pulse width 1 ns) with peak average energy density of ~3.5 x 10^5 W/cm^2 for different time. Involved procedure explained below.

2.3 Preparation of Amorphous Materials

There are several techniques that can be used to prepare materials in an amorphous state. In the present research work, melt-quenching method has been adopted to prepare the glassy alloys. The highly pure materials (99.999%) having the desired compositional ratio in accordance with their atomic percentage weight of elements have been weighted using an electronic balance and sealed in a quartz ampoule (length ~ 5cm, internal diameter ~ 8mm) in a vacuum of about 10^{-5} Torr. The sealed ampoules were kept inside a furnace where the temperature was raised at a rate of 4-5 K min^{-1} with frequent rocking to ensure the homogenization of the melt. The temperature and time for which ampoules had kept in furnace for different alloys have been given in Table 2.1 on next page. The rapid quenching has been done in ice cool water. After quenching, ingots of the quenched alloy were removed by breaking the ampoules. These ingots have been grinded into a fine powder using Pastel and Mortal. The following glassy alloys have been prepared in our present study:

Table 2.1: Composition and preparation condition of glassy alloys

Glassy system	***compositions***	***Preparation Condition***
$Se_{100-x}Te_x$	$Se_{96}Te_4$ $Se_{92}Te_8$ $Se_{88}Te_{12}$ $Se_{84}Te_{16}$	Temperature: 900 K Heating rate: 4 K / min Time: 10 hours
$Se_{96-x}Te_4Ga_x$	$Se_{96}Te_4Ga_0$ $Se_{94}Te_4Ga_2$	Temperature: 1173 K Heating rate: 5 K / min Time: 10 hours
$Se_{88}Te_{12-x}Al_x$	$Se_{88}Te_8Al_4$ $Se_{88}Te_6Al_6$ $Se_{88}Te_4Al_8$ $Se_{88}Te_2Al_{10}$	Temperature: 1100 K Heating rate: 4 K / min Time: 10 hours
$Se_{96-x}Te_4Hg_x$	$Se_{92}Te_4Hg_4$ $Se_{88}Te_4Hg_8$ $Se_{84}Te_4Hg_{12}$	Temperature: 900 K Heating rate: 4 K / min Time: 10 hours

2.4 Preparation of Amorphous Thin Films

We adopt vacuum evaporation technique of thin film deposition. The deposition unit consists of a vacuum chamber and a cabinet containing vacuum-pumping unit together with all the electrical components necessary for the coating process. Schematic diagram of bell jar shape Vacuum chamber has been shown in figure 2.1.

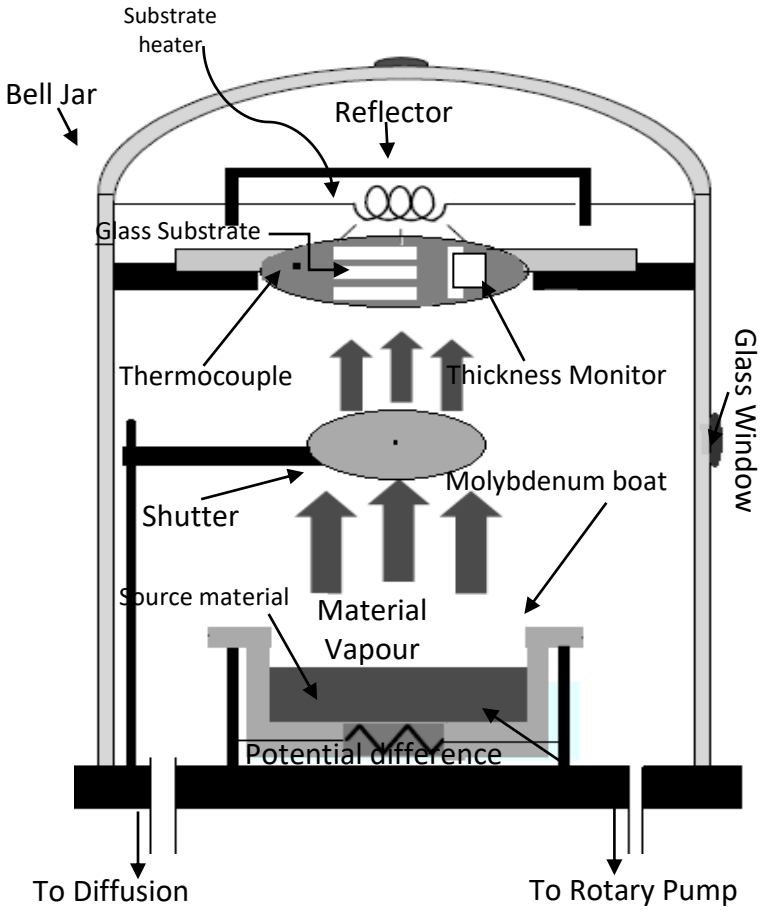

Figure 2.1: Schematic diagram of vacuum chamber

Vacuum chamber contains molybdenum boat where source material has to place. This boat connected with high voltage potential difference through which the boat can be heated till the alloy started to evaporate. Above the boat there is a shutter to control evaporation rate and thickness of deposited film with the help of single crystal thickness monitor mounted near substrate holder. Substrate holder connected with a substrate heater to vary substrate temperature as desired and a thermocouple to measure substrate temperature. To deposit thin film for all samples we use glass substrate at room temperature cleaned by ultrasonic bath using acetone and distill water. This chamber has two different inlet for rotary and diffusion

pump evacuation controlled by mechanical valve. The chamber is evacuated by diffusion pump and backed up by rotary pump. Diffusion pumps operate efficiently only at low pressures at both the inlet and outlet ports. Rotary pump used to evacuate the chamber to a pressure within the operating range of a diffusion pump; this is called the rough vacuum.

Once the chamber has been roughed, the mechanical valve is used to keep the outlet port of the diffusion pump at a low pressure, called the backing pressure. The pirani gauge is used to measure roughing and backing pressure (~ 0.5 to 10^{-3} Torr) and penning gauge is used to measure fine pressure (~ 10^{-2} to 10^{-6} Torr) in the chamber. An air admittance valve is fitted to the chamber pipeline to release the chamber vacuum. It admits a controlled flow of air into the chamber when required.

After achieving required vacuum pressure (~10^{-6} Torr) potential difference has been given to boat for heating and after a certain temperature material starts evaporating. Evaporated material of desired thickness has been deposited on pre-cleaned glass substrate. The thickness of all samples has been controlled by the help of single crystal thickness monitor and shutter. After evaporation, films of semiconductor compounds generally show heterogeneities of chemical composition and of crystal structure. The nature of these heterogeneities depends on the compound and on the evaporation method. Thin films of glassy semiconductor produced by evaporation show in general electrical and optical properties different from the corresponding properties of bulk materials.

2.5 Laser Irradiation System

High-energy beams like x-rays and lasers, both continuous wave (CW) and pulsed, are being increasingly used in a variety of material processing, manufacturing, and biomedical applications. Traditionally, most laser applications in material processing and medicine involve using of a CW laser; more recently, though, short pulsed lasers are being used in a variety of applications such as remote sensing, optical tomography, laser surgery, and ablation processes. Pulsed lasers have the additional ability to control the width and depth of heating as well as induce high heating or cooling rates because of higher peak powers and shorter time duration [53]. Short-pulsed lasers are thus being used increasingly for micromachining, welding, etching, cutting, and a variety of material processing applications [54–58].

In present study pulsed TEA N_2 laser has been used to irradiate all samples. TEA N_2 lasers emit Pulse radiation at a wavelength of 337.1 nm. One of the very basic characteristics of N_2 laser is that its radiation lasts in an extremely short time (5-10 ns), but its gain is very high. In present study TEA N_2 laser having pulse width 1 ns and peak power 100 kW has been used.

To irradiate prepared amorphous thin films, specially designed sample holder assembly attached with TEA N_2 laser unit has been used as shown in figure 2.2. This sample holder assembly consists of an adjustable lens and thin film holder with X-Y movement. Lens is used

to focus laser beam on sample holder with desired beam spot width. Thin film can be mounted in holder perpendicular to the laser beam at a desired distance from laser output head.

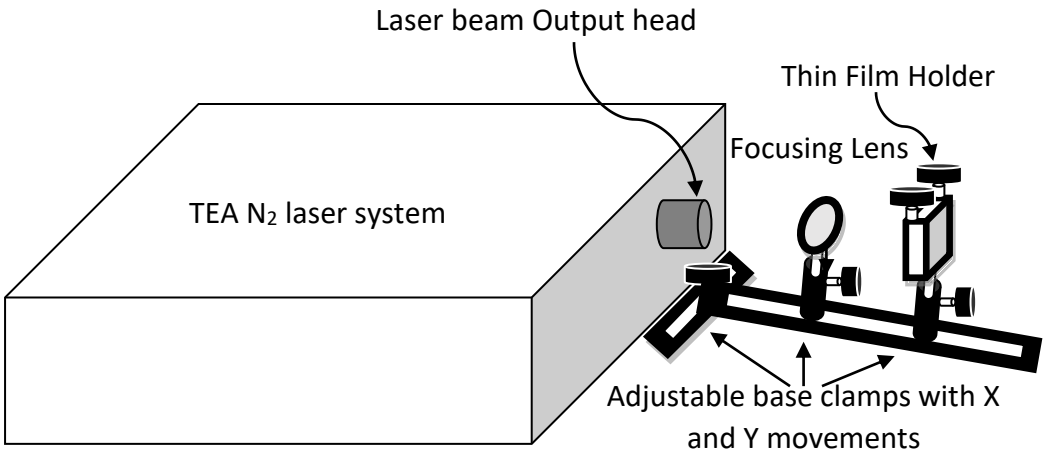

Figure 2.2: Layout of laser irradiation system.

In present study pulsed laser beam has been focused by lens perpendicular onto thin film mounted in sample holder, which kept at a distance of 15 cm from output laser head. For irradiation a spot of 6 mm diameter has been adjusted which irradiates thin film with an average peak power energy density of ~3.5 x 10^5 W/cm^2 for different times.

2.6 UV-Visible Spectroscopy

The word 'spectroscopy' is used as a collective term for all the analytical techniques based on the interaction of light and matter. Absorption or emission of photons occurs when a molecular system undergoes transition between energy states. When a photon is absorbed its energy is used to promote the molecular system to a higher energy state; if the molecular system is already in higher energy state, it can drop to a lower state with the emission of a photon. A graph of absorbance against wavelength gives the sample's absorption spectrum (Figure 2.3).

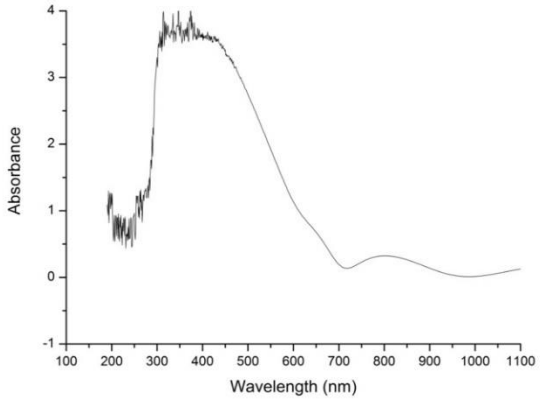

Figure 2.3: Graph of absorbance against wavelength

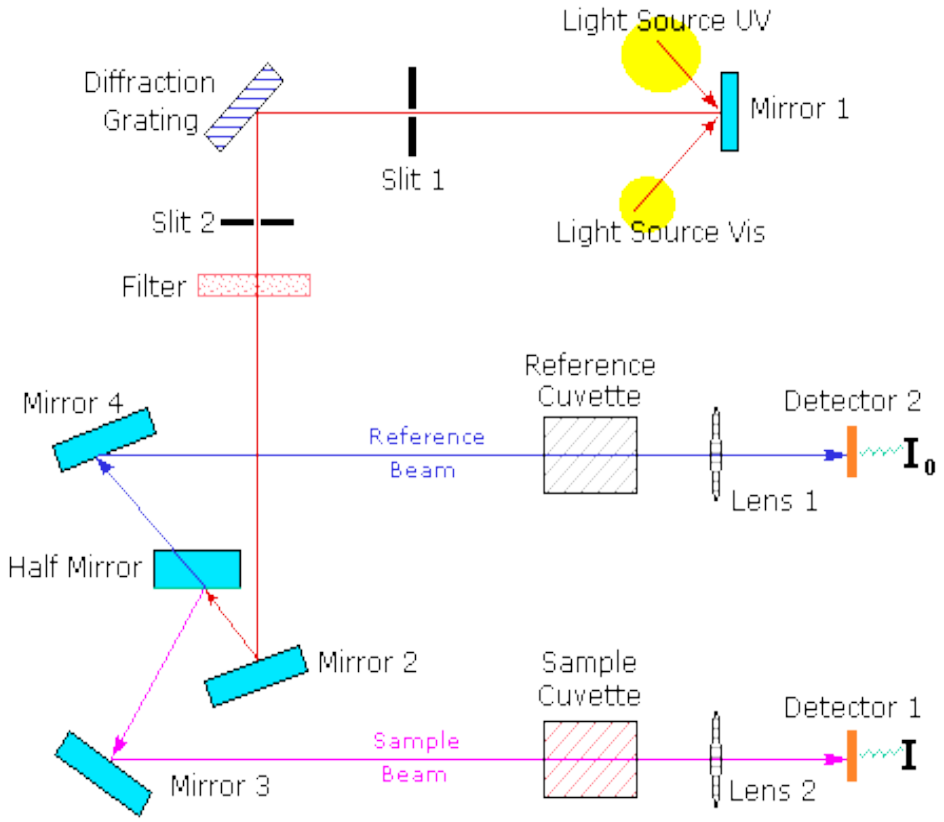

Figure 2.4: General layout of a double beam UV-visible spectrophotometer

The general layout of a UV-visible spectrometer is shown in figure 2.4. Source in wavelength range 190-1100 nm cannot get from a single lamp, and so a combination of two is used - a deuterium lamp for the UV part of the spectrum, and a tungsten / halogen lamp for the visible part. Most instruments are arranged to scan smoothly through the full structural range and switching from one source to the other can be achieved smoothly using a moving mirror, through in some instruments the light sources themselves are moved. The combined output electromagnetic radiation of these two bulbs is focussed on to a monochromator which can consist of a prism or a diffraction grating. A prism splits light into its component colours and a diffraction grating also does the same job, but more efficiently. This spreads out the spectral components, permitting a very narrow range from the whole spectrum (a tiny part of the range at a time) to be passed through a slit by gradually rotating the monochromator. The slit passes a finite bandwidth which must be 10 % of the natural bandwidth of the spectral line to be measured to avoid significant error in the peak intensity. Each monochromatic (single wavelength) beam in turn is split into two equal intensity beams by a half-mirrored device. One beam passes through the sample cell where sample, to be studied can mount using suitable sample holder. The other beam passes through the reference cell where reference used

in sample can mount. The intensities of these light beams are then measured by electronic detectors and compared. The intensity of the reference beam, which should have suffered little or no light absorption, is defined as I_0. The intensity of the sample beam is defined as I. Over a short period of time, the spectrometer automatically scans all the component wavelengths in the manner described. The ratio of I to I_0 is defined as Transmittance (T)

$$T = \frac{I}{I_0} \qquad (2.5)$$

The absorbance A, is related to the input and output intensities according to the Beer-Lambert law [59, 60] which is shown in equation

$$A = -\log T = -\log \frac{I}{I_0} \qquad (2.6)$$

The absorption of UV or visible radiation corresponds to the excitation of outer electrons. When an atom or molecule absorbs energy, electrons are promoted from their ground state to an excited state. In a molecule, the atoms can rotate and vibrate with respect to each other. These vibrations and rotations also have discrete energy levels, which can be considered as being packed on the top of each electronic energy level. In the present work the absorption spectra of thin films were collected by using Camspec M550 double beam UV-Visible Spectrophotometer shown in figure 2.5, in the range 190 to 1100 nm.

Figure 2.5: Camspec M550 double beam UV-visible spectrophotometer

2.7 Laser Irradiation Effect on Optical Properties of Chalcogenide Glassy Alloys.

Effect of laser irradiation on optical properties of Se-Te based glassy alloys having different additives as given in table 2.1 has been studied. For all samples thermally, evaporated amorphous thin film has been used. Obtained results before and after laser irradiation for all alloys have been explained below.

2.7.1 Effect of laser irradiation on optical properties of a-$Se_{100-x}Te_x$ thin films

(Radiation Effects & Defects in Solids;Vol. 166, No. 7, July 2011, 529–536)

The effect of laser irradiation on optical properties of thermally evaporated $Se_{100-x}Te_x$ (x = 8, 12, 16) chalcogenide thin films of thickness 300nm have been studied. The result shows that irradiation causes a shift in the optical gap. The results have been analyzed on the basis of laser irradiation-induced defects in the film. The width of the tail of localized state in the band gap has been evaluated using the Urbach edge method.

The amorphous thin films have been irradiated with TEA N_2 laser for 5, 10, 15 & 20 minutes having peak average energy density of ~3.5 x 10^5 W/cm^2. The optical spectrum has been measured as a function of wavelength (190-1100 nm) of incident light.

Measurement of the absorption coefficient (α) as a function of frequency (ν) provides a mean to determine the optical band gap (E_g) of thin film. The absorption coefficient has been calculated directly from the equation 2.1. Estimated values of the absorption coefficient (α) near the absorption edge for pristine and laser irradiated samples are given in table 2.2.

It has been observed that absorption coefficient increases with increasing irradiation time. Width of the band tail of the localized states in the band gap, also known as Urbach energy (E_U) has been calculated using equation 2.3. The width of the localized states depends on the degree of disorder and defects present in the amorphous structure. Magnitude of E_U has been calculated by taking slope of $\ln \alpha$ versus $h\nu$ curve. Value of E_U is very much larger than 0.05 eV; a minimum value that satisfies Urbach's formula. Estimated Urbach energy is shown in table 2.2 for all samples. Urbach energy increases with irradiation time which indicates decreasing in film crystallinity.

The optical band gap (E_g) have been measured by using equation 2.4 from the plot $(\alpha h\nu)^{1/2}$versus $h\nu$ by extrapolating the curves to $h\nu$ axis at $(\alpha h\nu)^{1/2} = 0$ for all samples before and after laser irradiation with different time as shown in figures 2.5 to 2.7.

Table 2.2: Optical parameters of $Se_{100-x}Te_x$ thin films at 600 nm

S.N.	Sample/ Exposure time	α ($10^4 cm^{-1}$)	k	E_U (meV)	E_g (eV)
1.	$Se_{92}Te_8$				
(a)	Pristine film	2.205±0.3	0 .1053	157	1.56±0.001
(b)	Exposure time				
(i)	5 minutes	2.344±0.3	0.1119	585	1.53±0.001
(ii)	10 minutes	2.238 ± 0.3	0.1069	948	1.50±0.001
(iii)	15 minutes	2.331±0.3	0.1114	1182	1.46±0.001
(iv)	20 minutes	1.376±0.3	0.0836	1360	1.41±0.001
2.	$Se_{88}Te_{12}$				
(a)	Pristine film	2.287±0.3	0 .1188	432	1.51±0.001
(b)	Exposure time				
(i)	5 minutes	2.487±0.3	0.1193	518	1.40±0.001
(ii)	10 minutes	2.497±0.3	0.1159	911	1.37±0.001
(iii)	15 minutes	2.425±0.3	0. 1245	955	1.34±0.001
(iv)	20 minutes	2.605±0.3	0.1341	1199	1.30±0.001
3.	$Se_{84}Te_{16}$				
(a)	Pristine film	3.121±0.3	0.1491	492	1.41±0.001
(b)	Exposure time				
(i)	5 minutes	3.247±0.3	0.1551	582	1.37±0.001
(ii)	10 minutes	3.051±0.3	0.1204	700	1.30±0.001
(iii)	15 minutes	3.256±0.3	0.1458	794	1.24±0.001
(iv)	20 minutes	3.267±0.3	0.1561	883	1.19±0.001

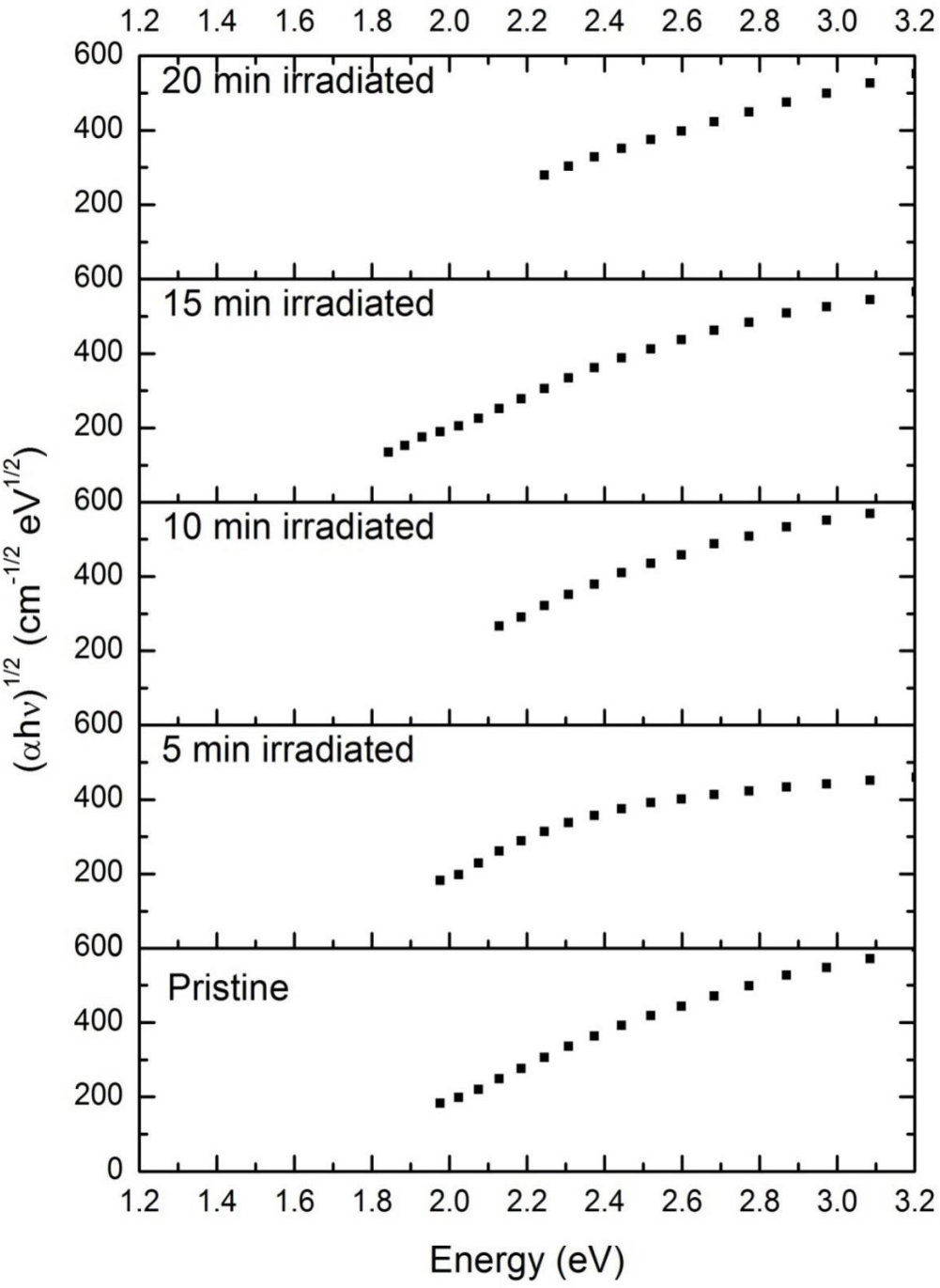

Figure 2.5: Variation of $(\alpha h\nu)^{1/2}$ with photon energy ($h\nu$) without and with laser irradiated $Se_{92}Te_8$ thin film.

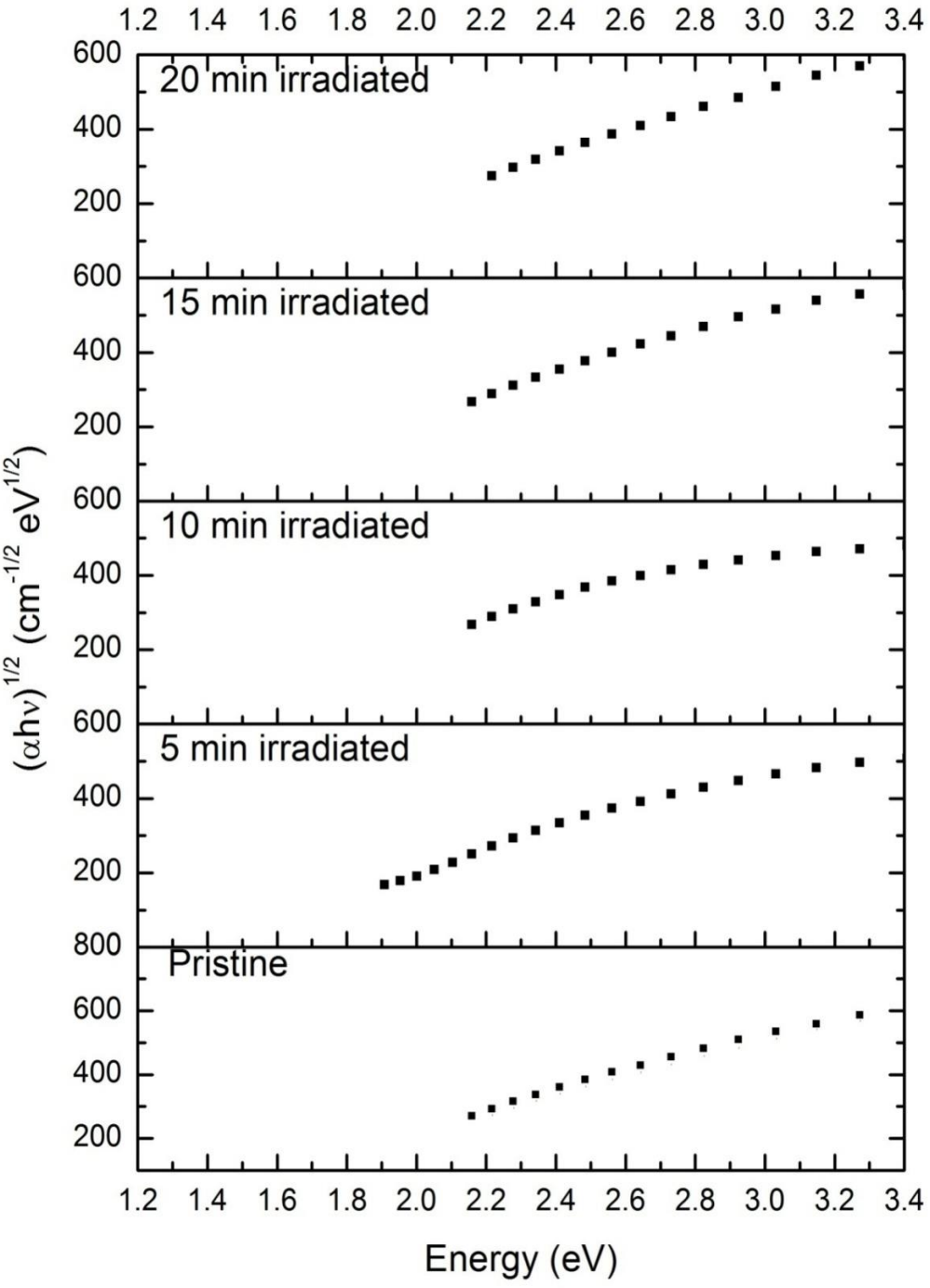

Figure 2.6: Variation of $(\alpha h\nu)^{1/2}$ with photon energy ($h\nu$) without and with laser irradiated $Se_{88}Te_{12}$ thin film.

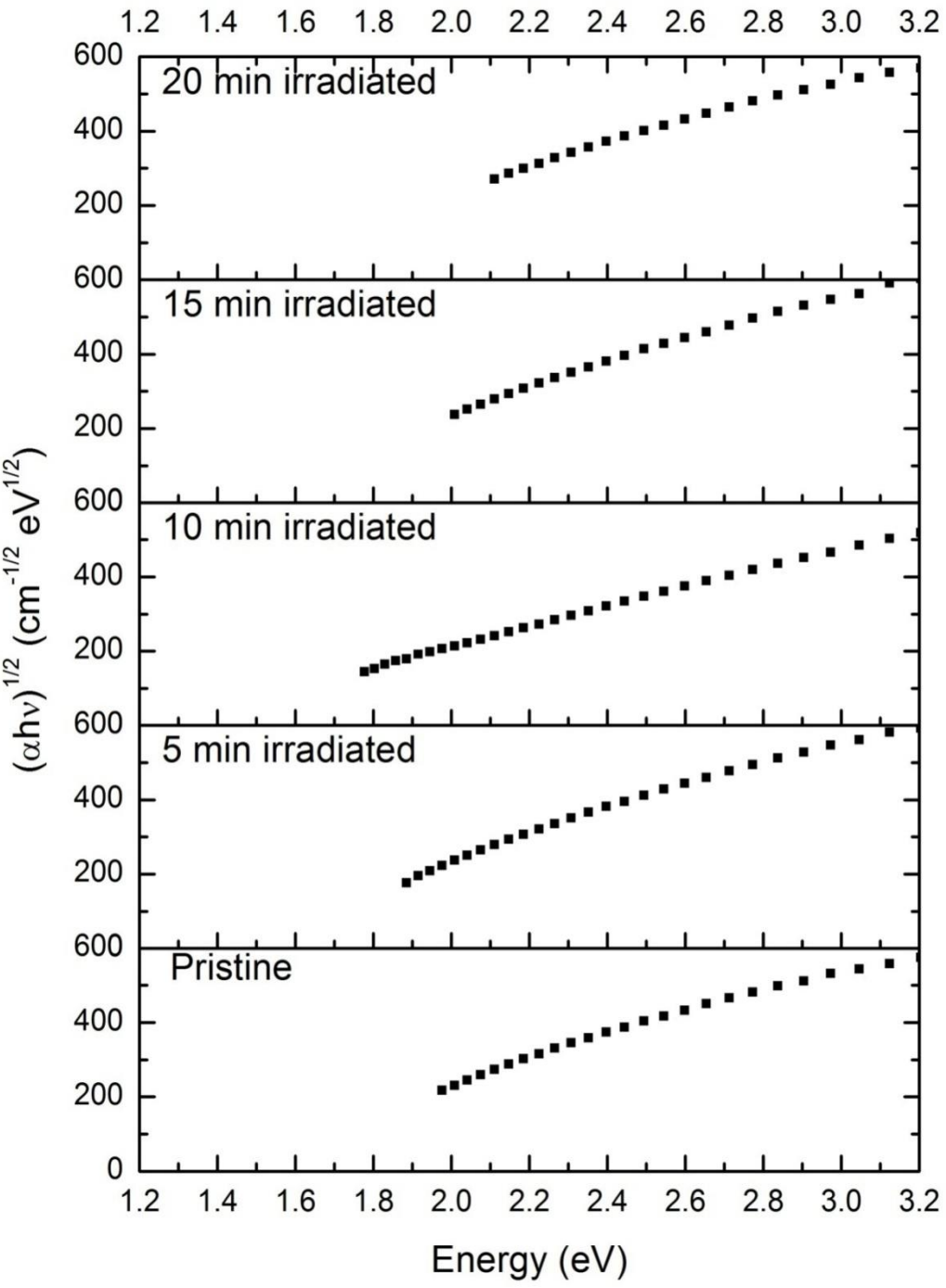

Figure 2.7: Variation of $(\alpha h\nu)^{1/2}$ with photon energy ($h\nu$) without and with laser irradiated $Se_{84}Te_{16}$ thin film.

During optical parameters estimation from absorption data the systematic error of instrument has been considered and respective uncertainties are given in table 2.2. The table shows that the optical energy gap decreases with increasing laser irradiation time as well as Te content in Se-Te alloy. Variation of optical band gap and Urbach energy with laser irradiation time are shown in figure 2.8.

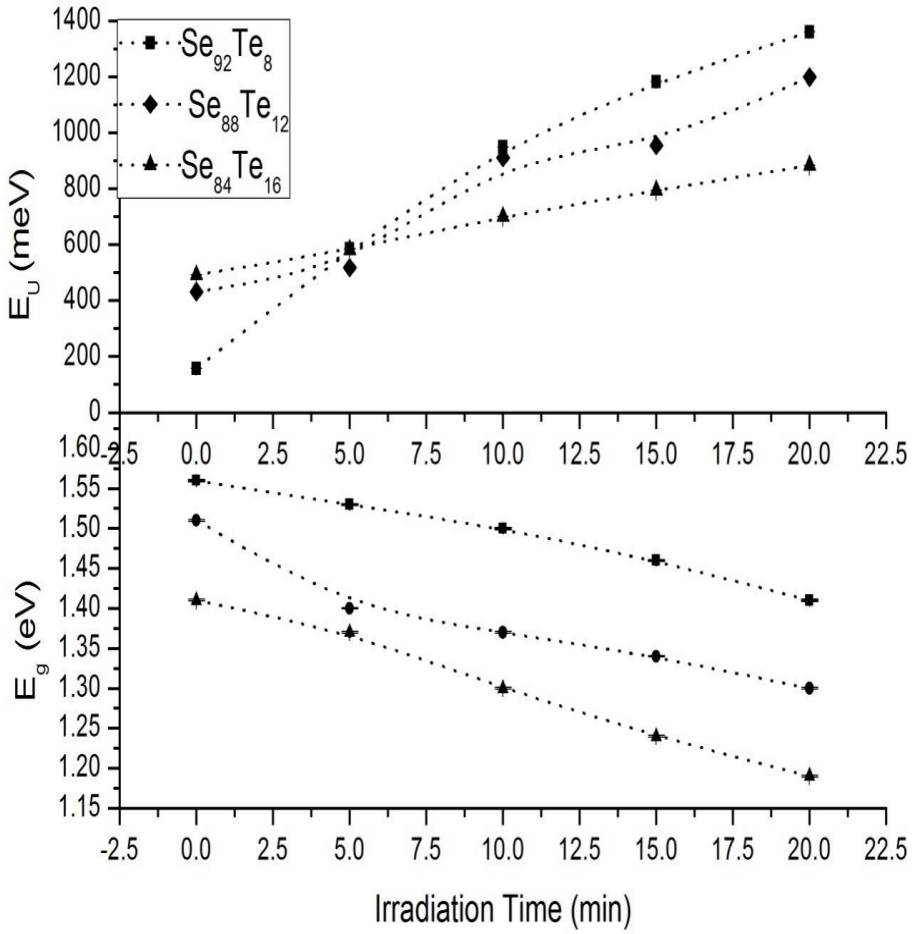

Figure 2.8: Variation of optical band gap (E_g) and Urbach energy (E_U) with laser irradiation time

Valance band of chalcogenide forms by lone pair orbital whereas the conduction band is formed by anti-bonding orbital [61]. The decrease in the energy gap has been explained by Kastner's suggestion [62] that, the lone pair electrons adjacent to electropositive atoms will have higher energies than close to electronegative atoms. Therefore, addition of more

electropositive atoms to the alloy may raise the energy of some lone pair state and hence to broaden the band into the forbidden gap. Se is more electronegative than Te, hence an increment of Te content in Se-Te alloy would expect to raise some lone pair states and broaden the valance band giving rise to additional absorption over a wide range. This may be responsible for the decrease in the optical energy gap by increasing Te content. Laser irradiation excites the electron from the lone pair of bonding state to higher energy states and hence vacancies created in these states. These vacancies are immediately filled by the outer electrons via Auger process. This induces more holes in the lone pair bonding orbital leading to a vacancy cascade process. This makes easier bond breaking and ionization of atoms and changes the local structure order of the amorphous network, which leads a decrease in the optical energy gap. Se-Te alloy regarded as a mixture of Se_8 rings, Se-Te mixed rings and Se-Te chain having different lengths. Se-Te covalent bond is stronger than the mean value of Se-Se and Te-Te bonds [63]. Therefore, Se-Te alloy tends to maximize the number of Se-Te bonds and the proportion of Se_8 rings decreases rapidly with the increases of Te content [64]. A strong covalent bond [65] existed between the atoms in the ring, whereas in between the chain only weak Van der Waal forces dominant. This makes it easy to break chains by laser irradiation and leads to an increment of disorder in the amorphous network. As a consequence of produced disorderness in the amorphous network, E_U increases because E_U strongly depends on the degree of disorder present in the amorphous structure. This effect is possibly responsible for the increase of absorption in the sample with increasing laser irradiation time as well as Te content. Hence the large influence of laser irradiation on the optical properties is connected with a higher degree of disorder in the alloy. Analysis of E_U also revealed an increment in the number of localized state into the gap. This will increase the transition probabilities through the localized state to the conduction band and consequently, the absorption coefficient (α) increases which lead shift of absorption edge toward lower energy. Hence the increase in transition probability due to disorder produced by laser irradiation leads to narrow the optical band gap of chalcogenide alloy. The extinction coefficient (k), which indicates the amount of absorption loss when the electromagnetic wave propagates through the material, has been calculated using well known relation [66-68]

$$k = \frac{\alpha\lambda}{4\pi} \qquad (2.7)$$

Where,α is absorption coefficient and λ is the corresponding wavelength. Extinction coefficient is frequency dependent. In the region of strong absorption, the interference fringes disappear [69] and near the absorption edge reflection coefficient are negligible and insignificant. Hence we choose a wavelength near the absorption edge to analyze the effect of laser irradiation and increase in Te content. The estimated values of the extinction coefficient before and after laser irradiation are given in table 2.2, and found to be increases with increasing the laser irradiation time.

The optical measurements of thin films indicate indirect allowed transition in Se-Te system. Analysis of the results reveals that the laser irradiation produces disorder in material, causing an increase in the number of localized states in the band gap. As a result tail energy width (E_U) increases and optical band gap (E_g) decreases with increasing irradiation time as well as Te content. It is also observed that absorption coefficient (α) and extinction coefficient (k) increases with laser irradiation time.

2.7.2 Effect of Laser Irradiation on the Optical Properties of Amorphous $Se_{96-x}Te_4Ga_x$ Thin Films

Amorphous $Se_{96}Te_4$ and $Se_{94}Te_4Ga_2$ thin films of thickness 400 nm have been prepared onto glass substrates by using thermal evaporation method. These thin films are irradiated by pulsed nitrogen laser upto~7min. The laser irradiation effect in the optical properties has been measured in the wavelength range 350-900 nm by spectrophotometer. It is found that optical band gap (E_g) is decrease in both samples after laser irradiation. It is also observed that addition of Ga increases optical band gap. The measurement of the absorption coefficient (α) as a function of frequency (ν) of the incident beam provides a mean to determine the band gap E_g of a material. The absorption coefficient α has been calculated directly from the absorbance against wavelength curve using equation 2.1. Figure 2.9 and figure 2.10 shows the variation α as a function of incident photon energy ($h\nu$) for $Se_{94-x}Te_4Ga_x$ films before and after irradiation. It is found that the value of absorption coefficient is decreases with increase Ga. The absorption coefficient of these films are high ($\approx 10^4$ cm^{-1}) and are given in table 2.3.

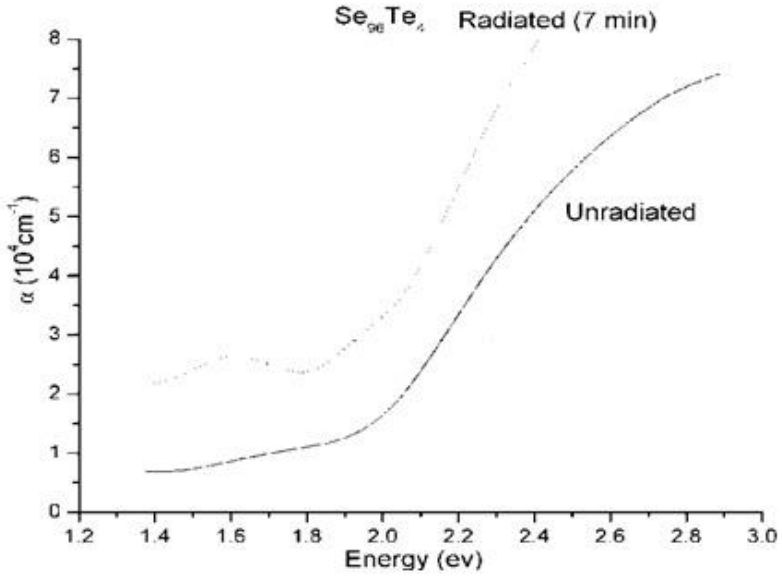

Figure 2.9: Variation of absorption coefficient (α) with incident photon energy ($h\nu$) for $Se_{96}Te_4$

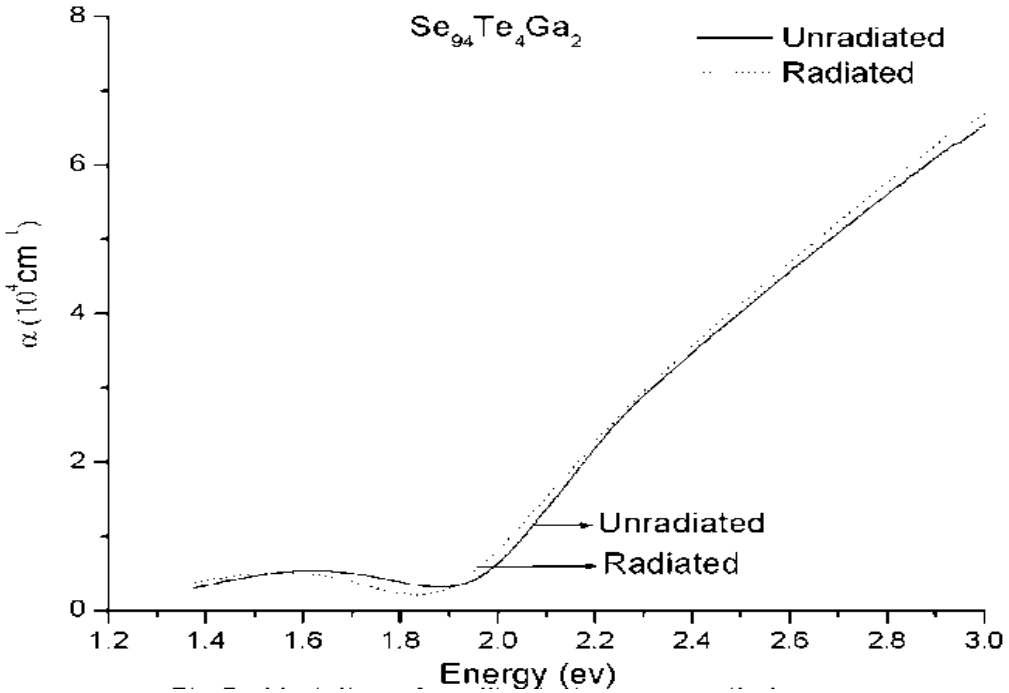

Figure 2.10: Variation of absorption coefficient (α) with incident photon energy (hν) for $Se_{94}Te_4Ga_2$

Table-2.3: Optical parameters of a -$Se_{96-x}Te_4Ga_x$ system at 600 nm.

S.N.	Sample	Un-irradiated			Irradiated		
		α (10^4cm^{-1})	k	E_g (eV)	α (10^4cm^{-1})	k	E_g (eV)
1	$Se_{96}Te_4$	2.0446	0.0977	1.59	3.7405	0.1787	1.47
2	$Se_{94}Te_4Ga_2$	1.5672	0.0505	1.80	1.0499	0.0502	1.76

The optical band gaps $Se_{96}Te_4$ and $Se_{94}Te_4Ga_2$ have been determined with the help of absorption spectra. The present system obeys indirect transition and indirect band gap has been calculated by well-known Tauc relation given in equation 2.4. Variation of $(\alpha h\nu)^{1/2}$ with photon energy (hν) for $Se_{96-x}Te_4Ga_x$ with and without irradiated films are shown in figure 2.11 and figure 2.12.

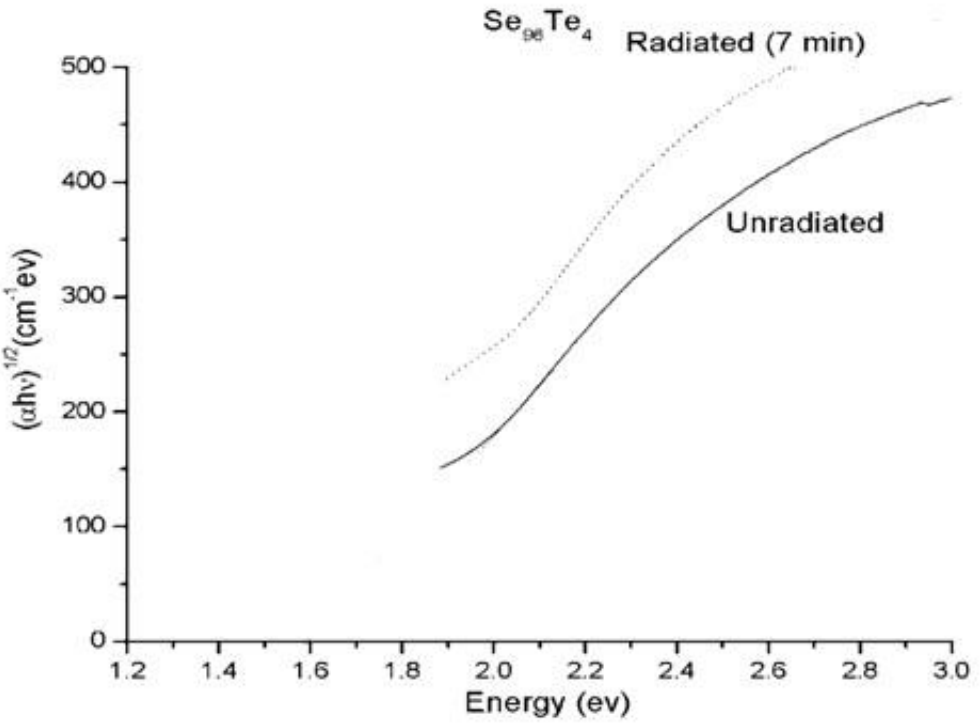

Figure 2.11: Variation of $(\alpha h\nu)^{1/2}$ with photon energy ($h\nu$) for $Se_{96}Te_4$

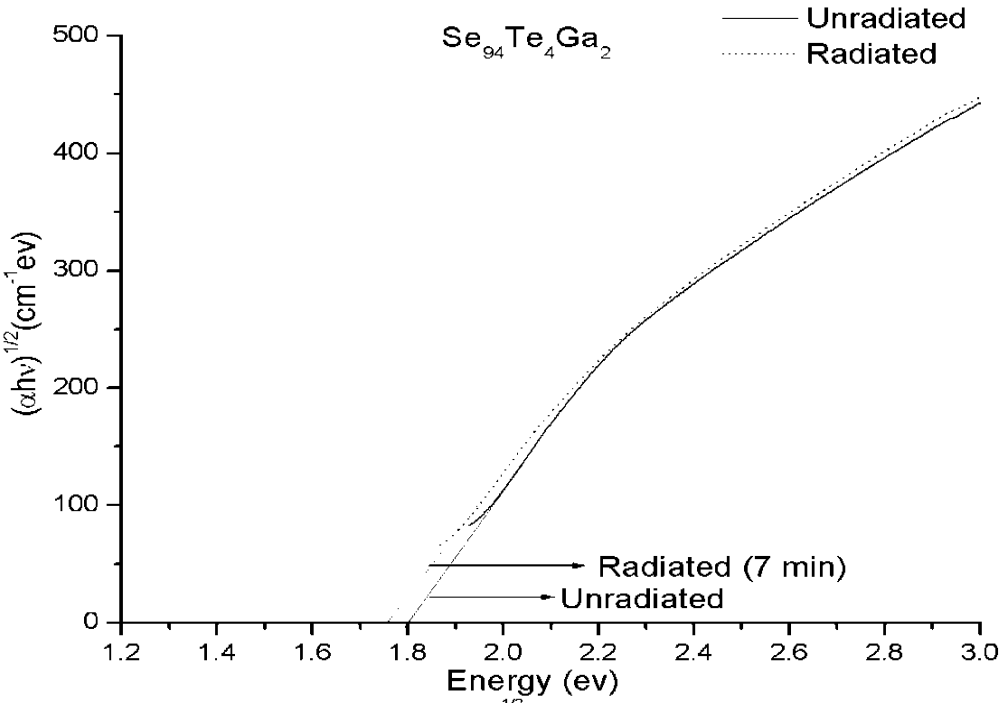

Figure 2.12: Variation of $(\alpha h\nu)^{1/2}$ with photon energy ($h\nu$) for $Se_{94}Te_4Ga_2$

The value of the indirect band gap has been determined by taking the intercept on the x-axis at y =0. It is clear that optical band gap decreases after irradiation, and calculated values are given in table 2.3. It is also clear from table that optical energy gap (E_g) increases with increase in Ga concentration in $Se_{96-x}Te_4Ga_x$ system. The increase of band gap suggests [70] a decrease in the density of localized states. In chalcogenide materials the lone pair orbital forms the valence band, whereas the conduction band is formed by the antibonding orbital [71].

The high-energy ions excite the electrons from the lone pair and bonding states to higher energy states. Vacancies created in these states are immediately filled by the outer electrons with Auger processes that in turn induce more holes in the lone pair and bonding orbital leading to a vacancy cascade process. In this process, bond breaking, or ionization of atoms is easier to occur which leads to a change in the local structure order of the amorphous network causing a decrease in the optical band gap. The increase in the optical band gap on the addition of Ga in the $Se_{96-x}Te_4Ga_x$ system may be explained on the basis of the model of density of states in amorphous solids proposed by Mott and Davis [72]. According to this model, the width of localized states near the mobility edges depends on the degree of disorder and defects presented in the amorphous structure. In particular, it is known that unsaturated bonds together with some saturated bonds [73] are produced as a result of insufficient number of atoms deposited in the amorphous films [74]. The unsaturated bonds are responsible for the formation of some defects in the films. Such defects produce localized states in the amorphous solids. Moreover, the increase in the optical band gap may be explained on the basis of the defects introduced in the system due to Ga incorporation. On the addition of Ga, Ga-Se bonding is developed, which introduces the larger number of defects in the system. The Ga-Se bond concentration increases with Ga concentration. It may also be due to the formation of an impurity band adjacent to a band and the formation of the tails of states extending the band into the mobility gap [75-78].

Extinction coefficient (k) has been calculated using the well-known relation using equation 2.7. Extinction coefficient (k) decreases as the Ga concentration increases and increases after irradiation in $Se_{94-x}Te_4Ga_{x-2}$ system. Variation of extinction coefficient with wavelength before and after irradiation has been shown in figure 2.13 and figure 2.14. Mott and Davis [72] have also been observed a similar trend for the thin films of the various other a-semiconductors. The values of extinction coefficient before and after irradiation are given in table 2.3.

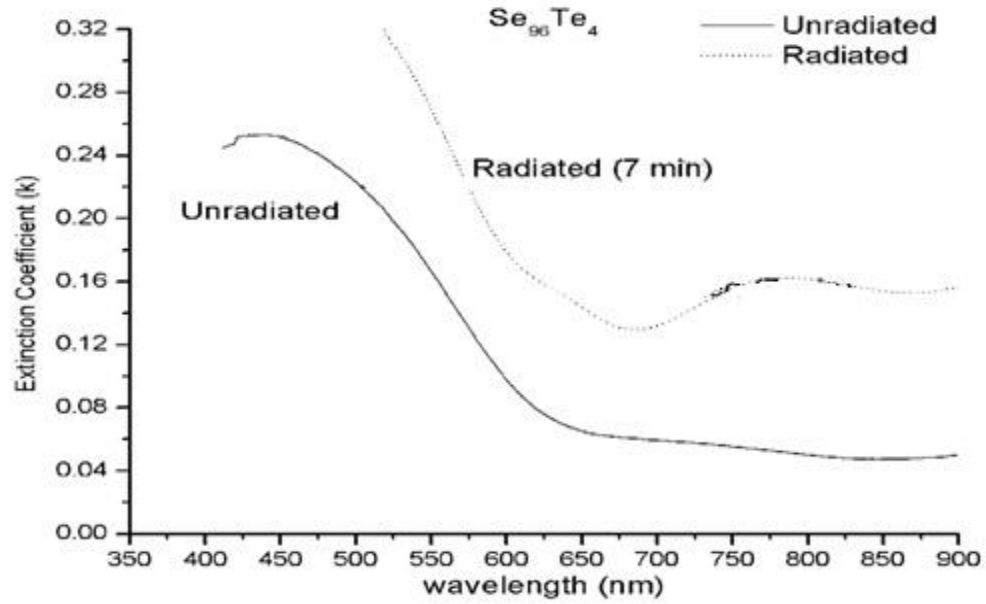

Figure 2.13: Variation of extinction coefficient with wavelength for $Se_{96}Te_4$

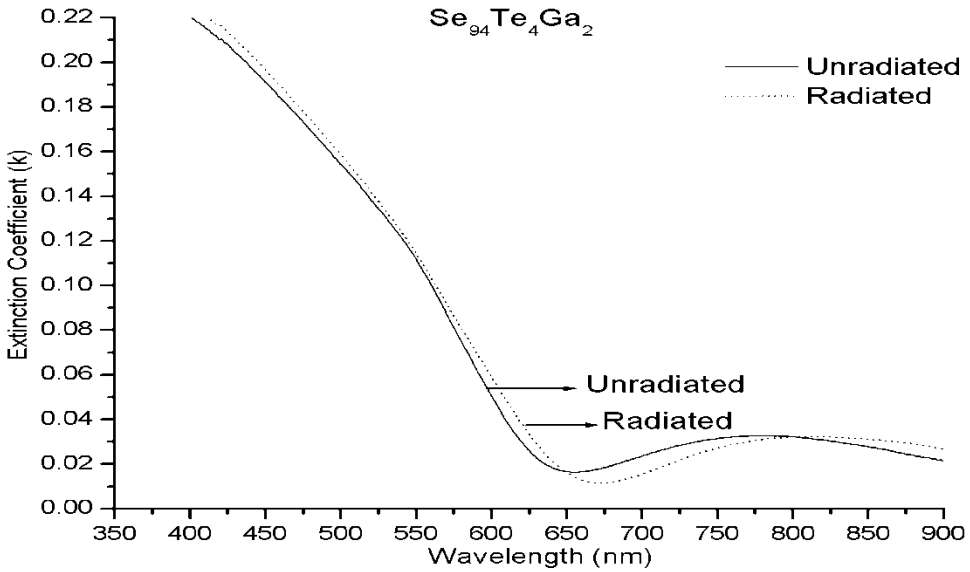

Figure 2.14: Variation of extinction coefficient with wavelength for $Se_{94}Te_4Ga_2$

Analysis of optical measurements of thin films indicates indirect allowed transition. The optical band gap (E_g) increases by increasing Ga content in $Se_{96-x}Te_4Ga_x$ system. It is observed that optical band gap (E_g) decreasing after laser irradiation. It is also observed that absorption coefficient (α) and extinction coefficient (k) decreases with Ga. The results have been

explained on the basis of enhanced valence band tailing caused by laser irradiation and the initiation of the Auger process upon irradiation.

2.7.3 Laser Irradiation Effect on the Optical Properties of Amorphous $Se_{88}Te_{12-x}Al_x$ Thin Films

The Laser Irradiation effect on Optical properties of $Se_{88}Te_{12-x}Al_x$ (where x= 4, 6, 8 and 10) thin films of thickness 300nm have been studied in wavelength range 190-1100 nm. The amorphous thin films have been irradiated with a pulsed Transverse Electrical Excitation at Atmospheric pressure (TEA) nitrogen laser for 5, 10, 15 & 20 minutes. Optical absorption measurements are widely used for studying disorder and defects in a-semiconductors. Optical absorption measurements are also very useful for studying the modifications of the density of states upon alloying. The optical absorption coefficient *(a)* has been calculated from the optical data using equation 2.1 and obtained value for all pristine and laser irradiated samples has been listed in table 2.4. The variation of absorption coefficient α as a function wavelength λ for all pristine thin films has been shown in figure 2.15.

It is observed that α decreases with increasing λ for all samples. For the pristine thin films Increase in aluminium concentration results in reduction of the absorption coefficient α in the range 300-650 nm. In the range 650-1100 nm the observed peak at 800 nm for $Se_{88}Te_8Al_4$ is disappear by increasing aluminium concentration. The effect of Al concentration on the absorption coefficient α is understandable in the light of the structural network. The clusters in $Se_{88}Te_{12-x}Al_x$ films are almost covered with the metallic additive Al, which results in high reflectance and decrease the observed absorption coefficient (α).

As described in chapter 1, in ChGs, a typical absorption edge can be broadly ascribed to any of the three processes: the high absorption region which determines the optical energy band gap, the exponential edge region which is strongly related to the structural randomness of the system; and the weak absorption tail which originates from defects and impurities. The plots of Tauc, Equation 2.4, for all the pristine and laser irradiated films are shown in Figures 2.16 - 2.19. The optical band gap (E_g) have been measured by extrapolating the curves to $h\nu$ axis at $(\alpha h\nu)^{1/2} = 0$ for all samples before and after laser irradiation with different time and obtained optical band gap E_g for all samples is given in Table 2.4.

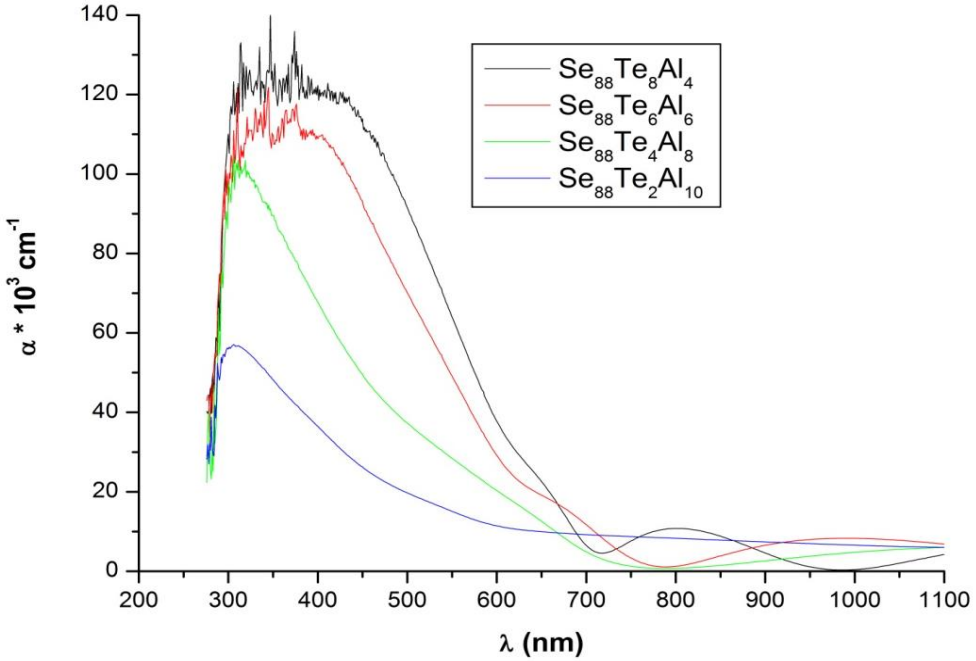

Figure 2.15: The variation of absorption coefficient α as a function of wavelength λ for different Al content.

During optical parameters estimation from absorption data the systematic error of instrument has been considered and respective uncertainties are shown in figure also given in table 2.4. The estimated optical energy gap decreases with increasing laser irradiation time as well as Al content in $Se_{88}Te_{12-x}Al_x$ alloy. The obtained optical band gap E_g shows that the increase in aluminium concentration results in decreasing the optical band gap which reveals an increase in the band broadening. The decrease in the energy gap has been explained by Kastner's suggestion [62] that, the lone pair electrons adjacent to electropositive atoms will have higher energies than close to electronegative atoms. Therefore, addition of more electropositive atoms to the alloy may raise the energy of some lone pair state and hence to broaden the band into the forbidden gap. Al is more electropositive than Se and Te, hence an increment of Al content in $Se_{88}Te_{12-x}Al_x$ alloy would expect to raise some lone pair states and broaden the valance band giving rise to additional absorption over a wide range. This may be responsible for the decrease in the optical energy gap by increasing Al content.

The estimated optical energy gap decreases with increasing laser irradiation time in Se-Te-Al alloy. This decrease of energy gap with radiation can be attributed to the variation of disorder and defects present in amorphous materials [79, 80]. The unsaturated bonds are responsible for the formation of some defects in the films. Such defects produce localized states in the amorphous solids. The presence of such localized states in the band structure is responsible for decreasing optical energy gap.

Table 2.4: Optical parameter @ 600 nm for $Se_{88}Te_{12-x}Al_x$

S.N.	Exposure time	α ($10^4 cm^{-1}$)	k	E_g (eV)
1.	**$Se_{88}Te_8Al_4$**			
(a)	Pristine film	1.351±0.3	0 .0645	1.62±0.001
(b)	Exposure time			
(i)	5 min	1.634±0.3	0.0780	1.59±0.001
(ii)	10 min	1.727±0.3	0.0824	1.54±0.001
(iii)	15 min	1.758±0.3	0.0839	1.48±0.001
(iv)	20 min	1.827±0.3	0.0872	1.39±0.001
2.	**$Se_{88}Te_6Al_6$**			
(a)	Pristine film	1.634±0.3	0 .0780	1.59±0.001
(b)	Exposure time			
(i)	5 min	1.726±0.3	0.0824	1.51±0.001
(ii)	10 min	1.737±0.3	0.0829	1.44±0.001
(iii)	15 min	1.751±0.3	0.0836	1.40±0.001
(iv)	20 min	2.059±0.3	0.0983	1.37±0.001
3.	**$Se_{88}Te_4Al_8$**			
(a)	Pristine film	1.604±0.3	0 .0766	1.56±0.001
(b)	Exposure time			
(i)	5 min	1.659±0.3	0.0792	1.50±0.001
(ii)	10 min	1.668±0.3	0.0796	1.45±0.001
(iii)	15 min	1.707±0.3	0.0815	1.40±0.001
(iv)	20 min	2.051±0.3	0.0979	1.34±0.001
4.	**$Se_{88}Te_2Al_{10}$**			
(a)	Pristine film	1.674±0.3	0 .0799	1.52±0.001
(b)	Exposure time			
(i)	5 min	1.959±0.3	0.0935	1.50±0.001
(ii)	10 min	1.759±0.3	0.0936	1.47±0.001
(iii)	15 min	1.827±0.3	0.0839	1.46±0.001
(iv)	20 min	1.828±0.3	0.0872	1.46±0.001

The unsaturated defects produce a large number of unsaturated bonds when get irradiated by laser. The increase in the number of unsaturated defects increases the density of localized states in the band structure [81] and consequently decreases the optical energy gap E_g [82]. Light-induced changes are favored in ChGs due to their structural flexibility (low coordination of chalcogens) and also due to their high-lying lone-pair p states in their valence bands [83] *T*he decrease in optical gap of Se-Te-Al thin films by laser irradiation may be explained on the basis of bonds distribution model suggested by Golovchak et al. [84, 85] According to them,

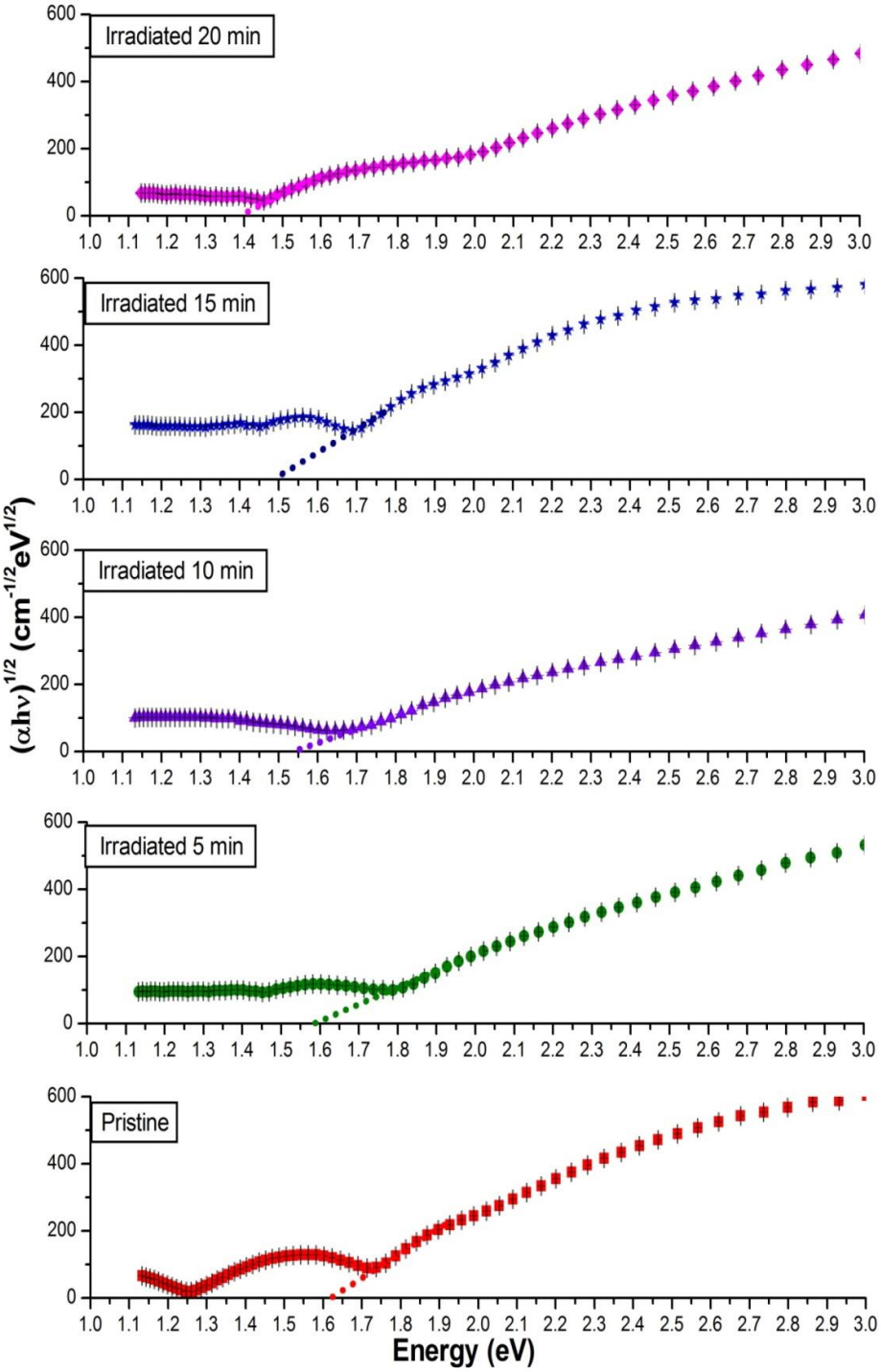

Figure 2.16: Variation of $(\alpha h\nu)^{1/2}$ with photon energy (hν) without and with laser irradiated $Se_{88}Te_8Al_4$ thin film.

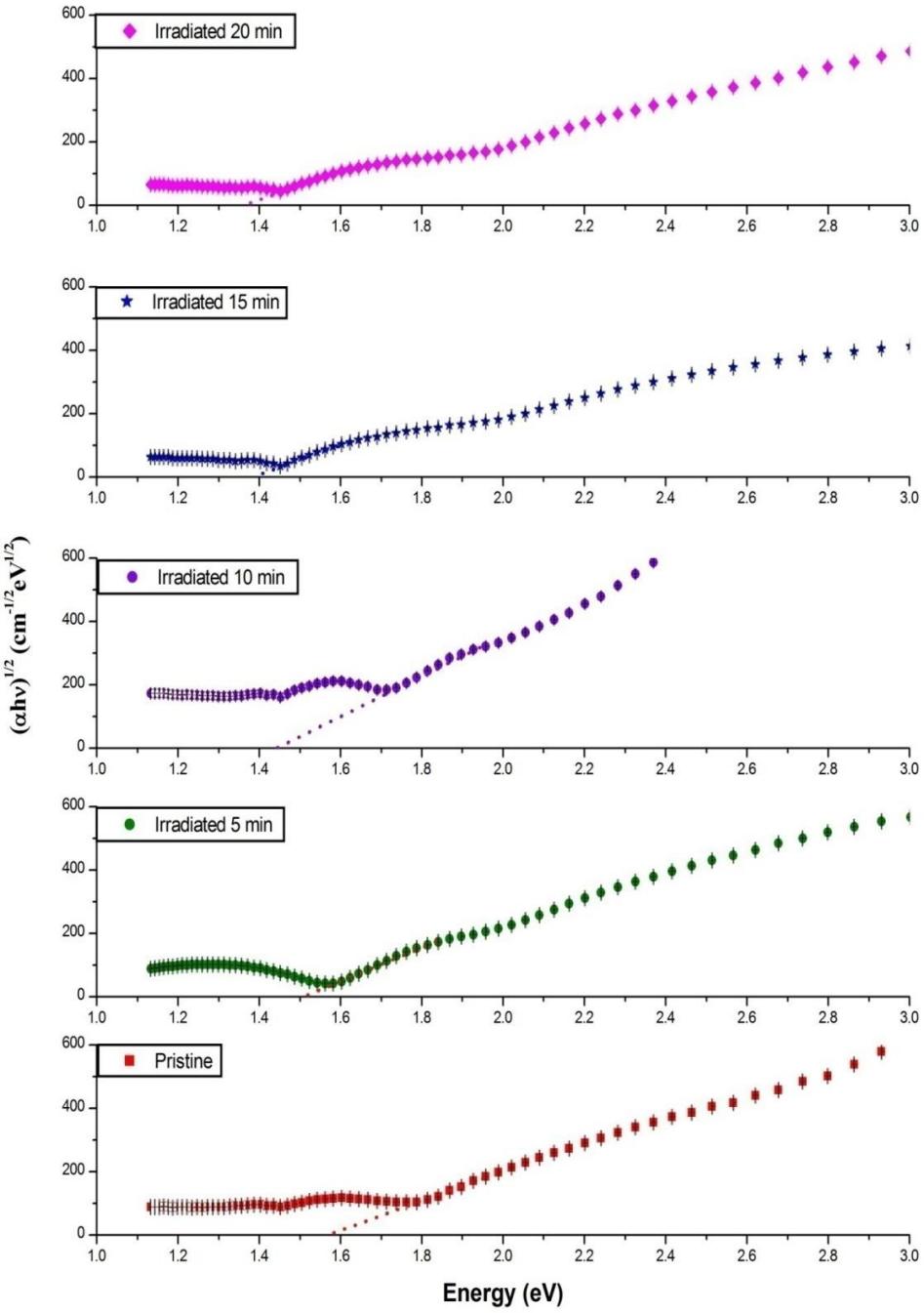

Figure 2.17: Variation of $(\alpha h\nu)^{1/2}$ with photon energy ($h\nu$) without and with laser irradiated $Se_{88}Te_6Al_6$ thin film.

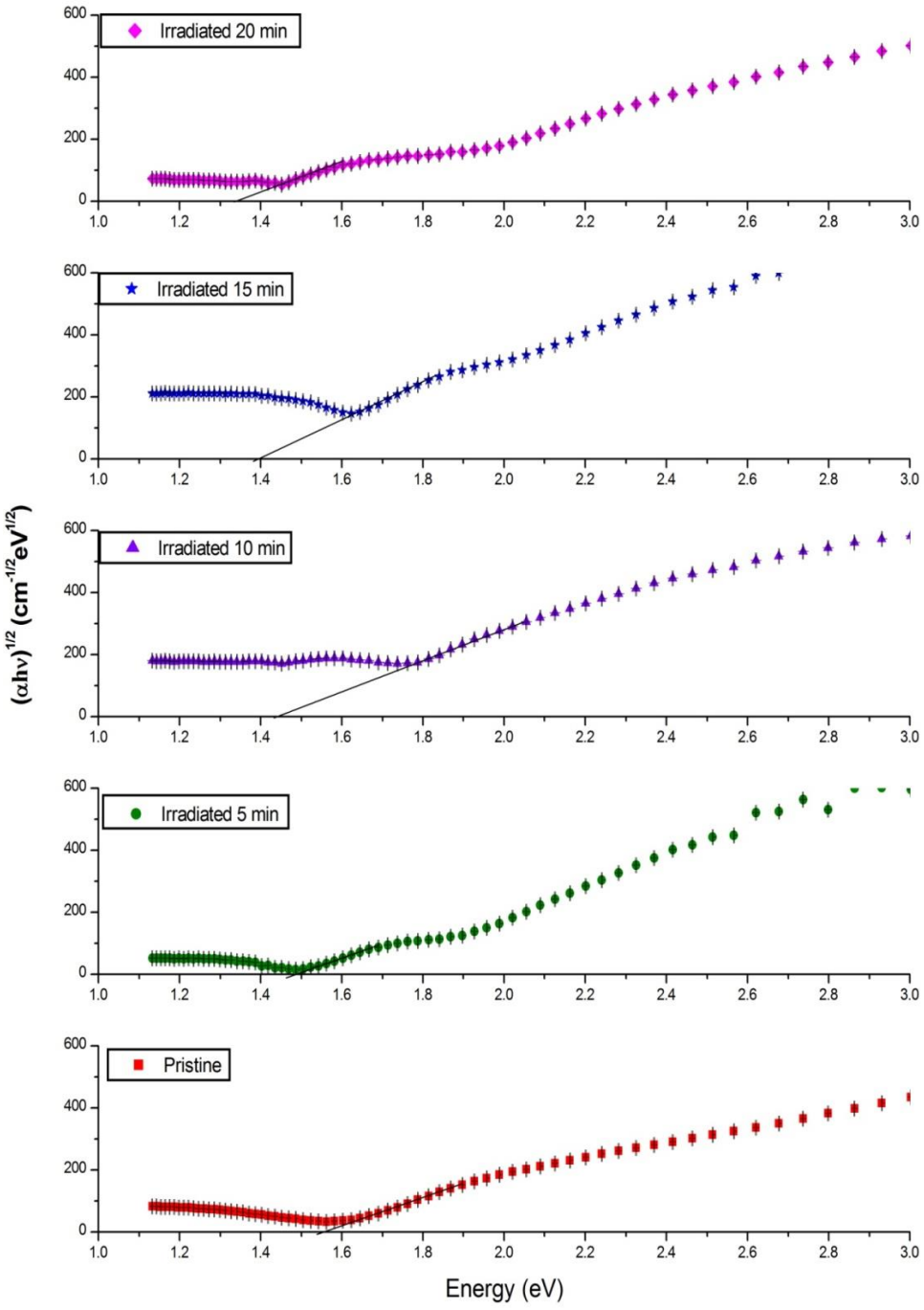

Figure 2.18: Variation of $(\alpha h\nu)^{1/2}$ with photon energy ($h\nu$) without and with laser irradiated $Se_{88}Te_4Al_8$ thin film.

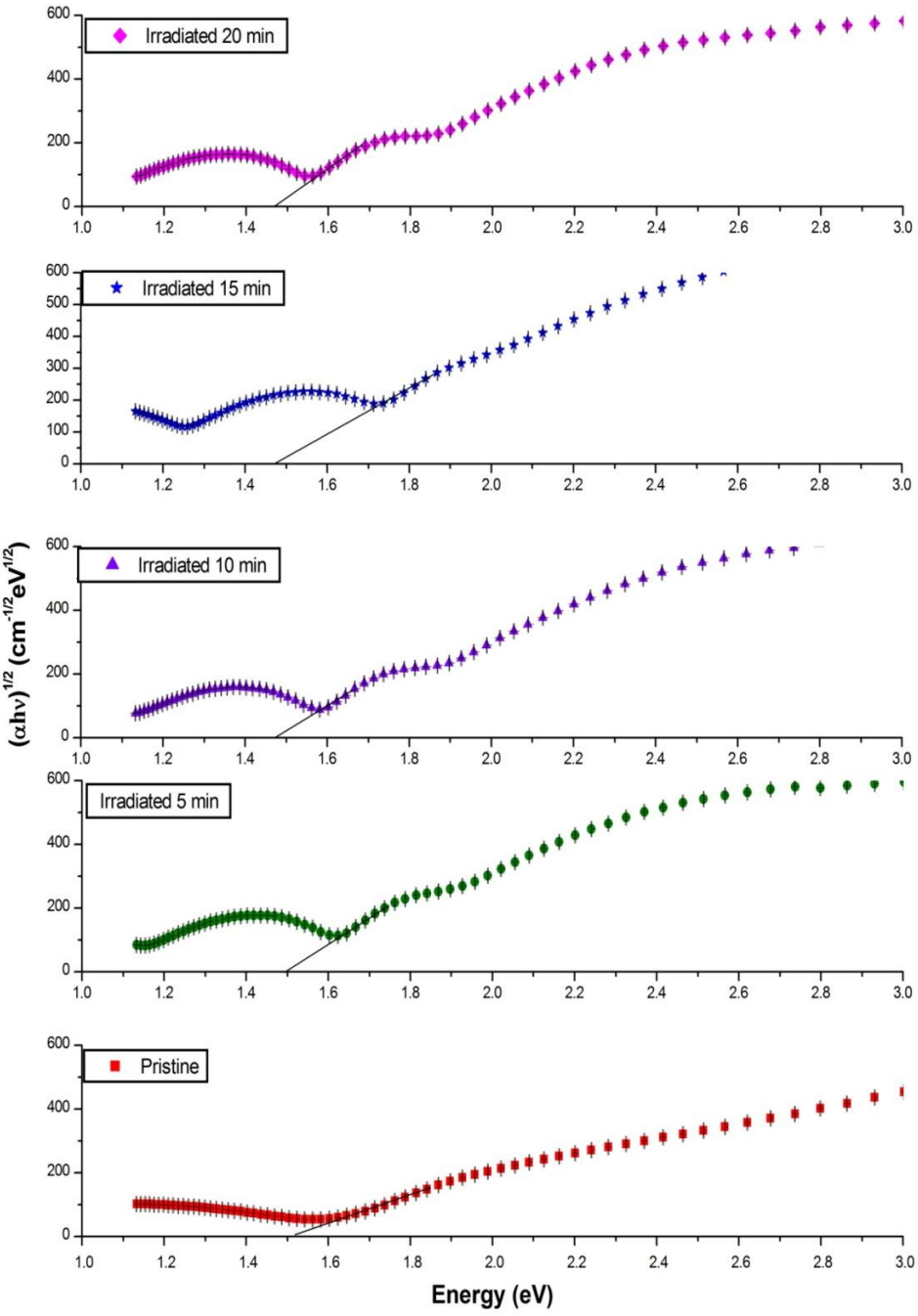

Figure 2.19: Variation of $(\alpha h\nu)^{1/2}$ with photon energy ($h\nu$) without and with laser irradiated $Se_{88}Te_2Al_{10}$ thin film.

it is assumed that chalcogen located 1p electrons as well as s-electrons of covalent bonds are excited. However, these electronic disturbances are not strongly localized, but decay giving rise to significant atomic displacements within the whole glass network with a new distribution of bonds. It is more likely that the change takes place in the chains, that is, the bonds within the chains may be broken and built between chains. It is mentioned that Se-Te bonds have bond energy less than that of Se–Al bonds, so it is expected that Se–Te bonds are more sensitive to laser irradiation. Therefore, upon laser irradiation some of Se–Te bonds are broken leading to the formation of Te–Te homopolar bonds, because of their low energy of formation [86]. This process allows the formation of defects which produce localized states that change the effective Fermi level due to an increase in carrier concentrations. This increase in carriers in localized states will lead to a decrease in the transition probabilities into the extended states, resulting in additional absorption and reduction in the gap [87, 88]. Further it has been observed that alloy with higher concentration of aluminum that is $Se_{88}Te_2Al_{10}$ does not show significant change upon irradiation time after 10 mins. Glasses with a higher content of Al have less Se-Te bond than Se-Al bond and consequently less sensitive to laser irradiation and not easy to create more defect states. It confirmed that the changes of optical properties for alloy with a higher content of aluminium are less sensitive to Laser irradiation. It suggests that Se-Al bond is stronger and less flexible, and accordingly, cannot readily influence by laser irradiation. The extinction coefficient (k), which indicates the amount of absorption loss when the electromagnetic wave propagates through the material, has been calculated using well known equation 2.7. Extinction coefficient is frequency dependent. In the region of strong absorption, the interference fringes disappear [69] and near the absorption edge reflection coefficient are negligible and insignificant. Hence, we choose a wavelength near the absorption edge to analyze the effect of laser irradiation and Al content. The estimated values of the extinction coefficient before and after laser irradiation are given in table 2.4 and found to be increases with increasing the laser irradiation time.

The optical measurements of thin films indicate indirect allowed transition in Se-Te-Al system. Analysis of the results reveals that the laser irradiation produces disorder in material, causing an increase in the number of localized states in the band gap. As a result optical band gap (E_g) decreases with increasing irradiation time as well as Al content. However laser irradiation does not show significant effect at higher Al concentration (10%). It might be due to lack of weak Se-Te bond as Te content decreases with increasing Al content. It concludes that alloy with rich Al content is more stable and laser irradiation cannot affect it. It is also observed that absorption coefficient (α) and extinction coefficient (k) increases with laser irradiation time.

2.7.4 Laser Irradiation Effect on the Optical Properties of Amorphous $Se_{96-x}Te_4Hg_x$ Thin Films

The effect of laser irradiation on optical properties of amorphous $Se_{96-x}Te_4Hg_x$ (x = 8, 12, 16) thin films have been studied. Thin films of thickness 300 nm have been deposited on glass substrate by thermal evaporation unit. The result shows that irradiation causes a red shift in the absorption edge and hence optical band gap decreases with increasing irradiation time. The results have been analyzed on the basis of laser irradiation-induced defects in the film. Furthermore, optical band gap has found to be decrease by increasing Hg concentration and Eg decreases rapidly with higher concentration of Hg. The amorphous thin films have been irradiated with TEA N_2 laser for 5, 10, 15 & 20 minutes having peak average energy density of ~3.5 x 10^5 W/cm^2. The optical spectrum has been measured as a function of wavelength (190-1100 nm) of incident light.

Optical absorption coefficient (*a)* has been calculated directly from the Absorption spectra using equation 2.1 and obtained value for all pristine and laser irradiated samples has been listed in table 2.5. The variation of absorption coefficient (α) as a function wavelength (λ) for all pristine thin films shows that α decreases with increasing λ for all samples as shown in figure 2.20. For the pristine thin films Increase in Hg concentration results in reduction of the absorption coefficient (α)in the range 290-580 nm and then its increases with increasing Hg concentration in the range of 580-800 nm. The effect of Hg concentration on the absorption coefficient (α) can be explained by considering structural network. Furthermore, α increases with increasing irradiation time. The optical band gap (E_g) have been measured by extrapolating the curves of Tauc plots [49] to $h\nu$ axis at $(\alpha h\nu)^{1/2} = 0$ for all the pristine and laser irradiated films and shown in Figures 2.21 to 2.23. Estimated optical band gap E_g for all samples are given in table 2.5.

During optical parameters estimation from absorption data the systematic error of instrument has been considered and respective uncertainties are shown in figure also given in table 2.5. Result shows that the optical energy gap decreases with increasing laser irradiation time as well as Hg content in Se-Te-Hg alloy. It can be clearly seen that energy band gap decreases rapidly with higher Hg concentration. It indicates that increase in mercury concentration results in rapid increase in the band broadening. Decrease of energy gap with radiation attributed to the variation of disorder and defects present in amorphous materials [79, 80]. The unsaturated bonds are responsible to produce localized defect states in the band structure of the amorphous solids. The presence of such localized states in the band structure is responsible for decreasing optical energy gap.

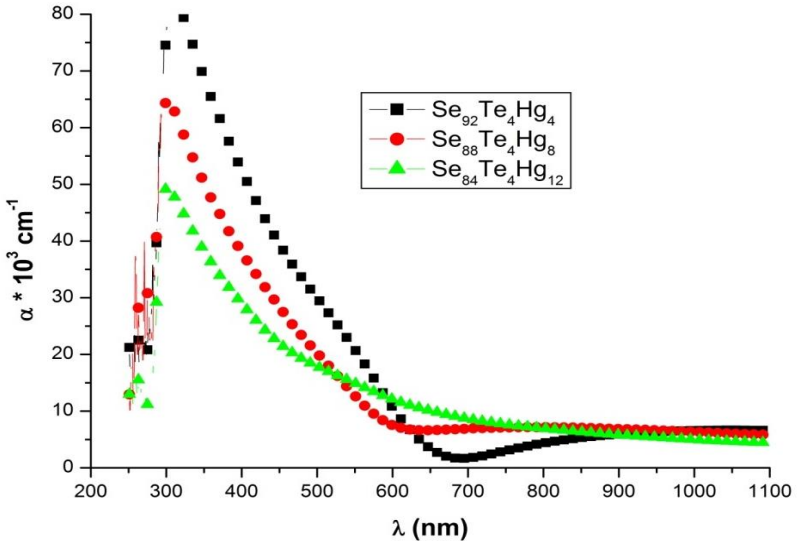

Figure 2.20: The variation of absorption coefficient α as a function of wavelength λ for different Hg content.

Table 2.5: Optical parameter @ 600 nm for $Se_{96-x}Te_4Hg_x$

S.N.	Exposure time	α ($10^4 cm^{-1}$)	k	E_g (eV)
1.	**$Se_{92}Te_4Hg_4$**			
(a)	Pristine film	0.752±0.3	0 .0359	1.71±0.001
(b)	Exposure time			
(i)	5 min	0.782±0.3	0.0374	1.66±0.001
(ii)	10 min	1.001±0.3	0.0478	1.64±0.001
(iii)	15 min	1.077±0.3	0.0515	1.60±0.001
(iv)	20 min	1.079±0.3	0.0515	1.56±0.001
2.	**$Se_{88}Te_4Hg_8$**			
(a)	Pristine film	1.067±0.3	0 .0509	1.69±0.001
(b)	Exposure time			
(i)	5 min	1.297±0.3	0.0620	1.67±0.001
(ii)	10 min	1.413±0.3	0.0675	1.64±0.001
(iii)	15 min	1.542±0.3	0.0736	1.62±0.001
(iv)	20 min	1.599±0.3	0.0764	1.60±0.001
3.	**$Se_{84}Te_4Hg_{12}$**			
(a)	Pristine film	1.109±0.3	0.0530	1.24±0.001
(b)	Exposure time			
(i)	5 min	1.124 ±0.3	0.0537	1.21±0.001
(ii)	10 min	1.164±0.3	0.0556	1.02±0.001
(iii)	15 min	1.208±0.3	0 .5773	1.00±0.001
(iv)	20 min	1.339±0.3	0.0639	0.92±0.001

The increase in the number of unsaturated defects increases the density of localized states in the band structure [81] and consequently decreases the optical energy gap E_g. [82]. Further, study of photoconductivity suggests that increase in Hg concentration also responsible to produce defect states and hence, availability of more localized defect state as found in earlier study of laser irradiation effect favored in ChGs due to their structural flexibility and also due to their high-lying lone-pair p states in their valence bands [83]. *T*he decrease in optical gap of Se-Te-Hg thin films by laser irradiation may be explained on the basis of bonds distribution model suggested by Golovchak et al. [84-86] that the bonds within the chains may be broken and change takes place in between chains.

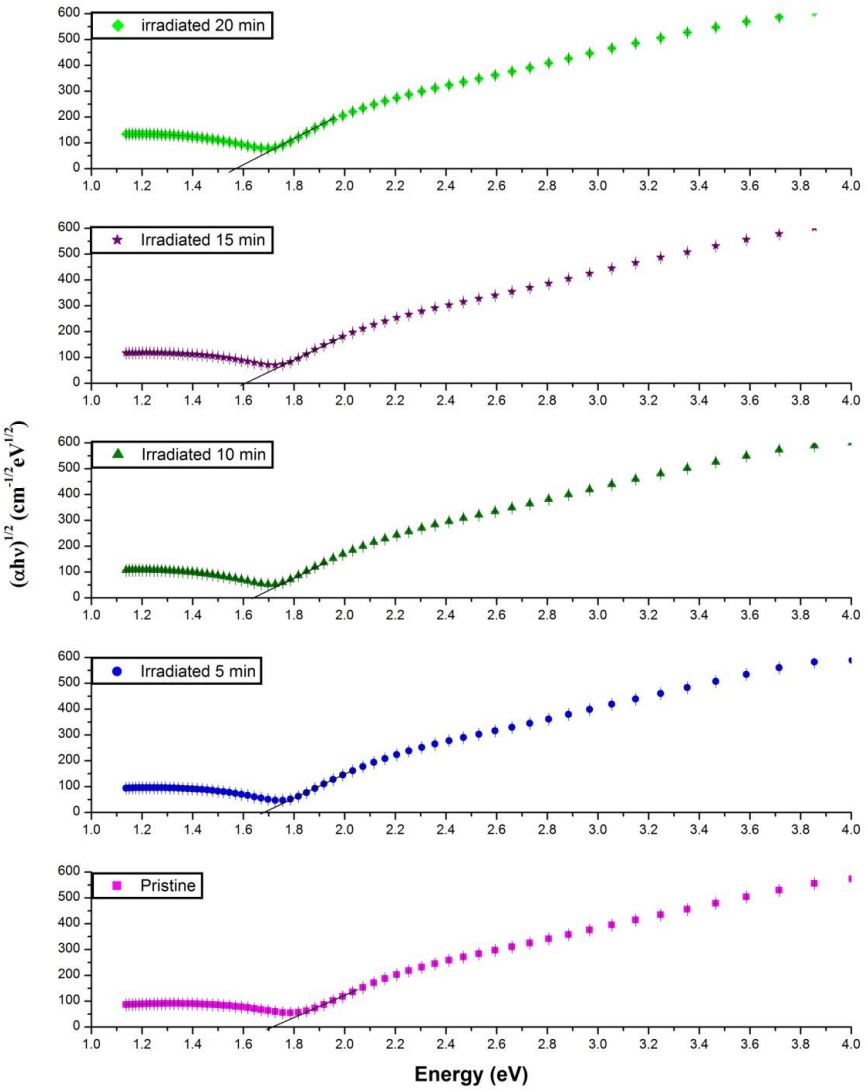

Figure 2.21: Variation of $(\alpha h\nu)^{1/2}$ with photon energy ($h\nu$) without and with laser irradiated $Se_{92}Te_4Hg_4$ thin film.

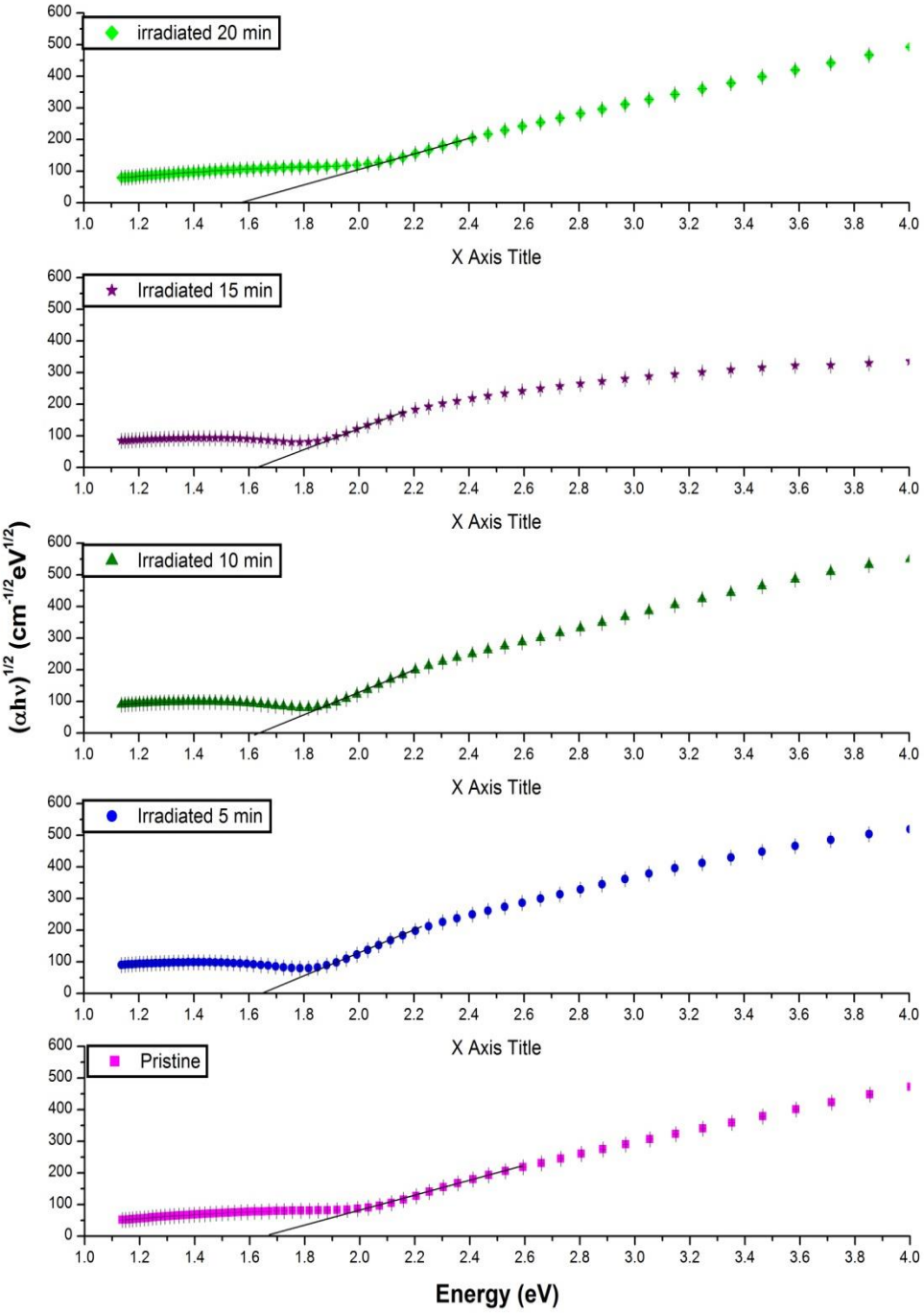

Figure 2.22: Variation of $(\alpha h\nu)^{1/2}$ with photon energy ($h\nu$) without and with laser irradiated $Se_{88}Te_4Hg_8$ thin film.

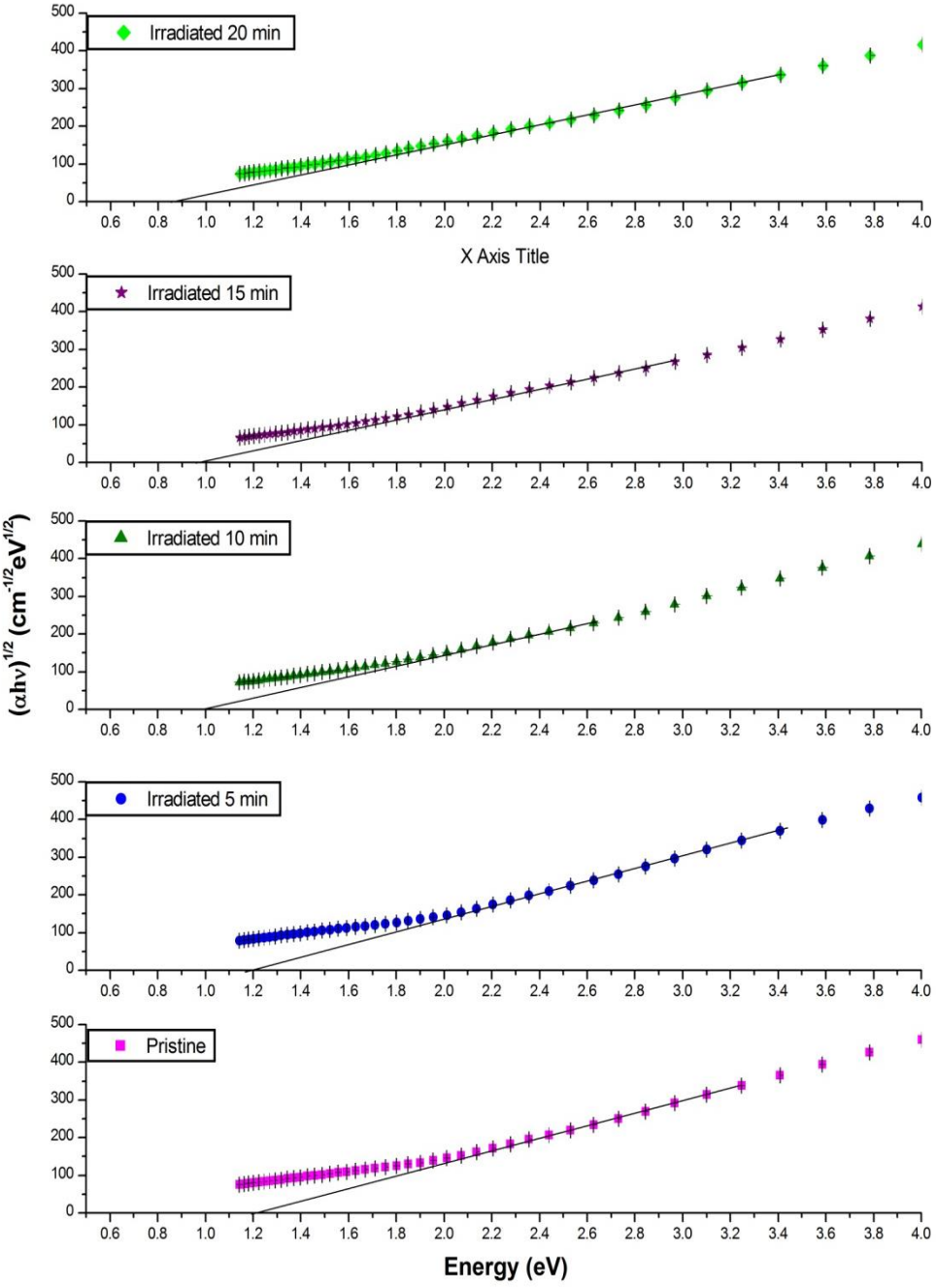

Figure 2.23: Variation of $(\alpha h\nu)^{1/2}$ with photon energy ($h\nu$) without and with laser irradiated $Se_{84}Te_4Hg_{12}$ thin film.

In the view of bond distribution model decrease in energy band gap with addition of Hg content and laser irradiation can be expected. Increase in Hg concentration favored availability of more Hg-Se bonds in the alloy. Since Hg-Se bond is weaker in comparison of other bonds present in the alloy and so easy to be break by laser irradiation. With increasing of Hg concentration more weak bonds would be available to be broken and hence the chance of the formation of defects increases. Due to this, availability of more localized states increases with increasing Hg content, which might be a reason to show strong effect of irradiation with higher Hg concentration in comparison of composition with less Hg concentration. It confirmed that the Se-Te based alloy with higher content of Hg is more sensitive to Laser irradiation.

Amount of absorption loss when the electromagnetic wave propagates through the material i.e. extinction coefficient has been calculated using well known equation 2.7. As mentioned earlier that extinction coefficient is frequency dependent. In the region of strong absorption, the interference fringes disappear and near the absorption edge reflection coefficient are negligible and insignificant. Hence, we choose a wavelength near the absorption edge to analyze the effect of laser irradiation and Hg content on absorption coefficient and extinction coefficient. The estimated values of the extinction coefficient before and after laser irradiation are given in table 2.5 and found to be increases with increasing the laser irradiation time.

Optical absorption measurements of thin films show indirect allowed transition in Se-Te-Hg system. Result shows that the laser irradiation produces disorder in the material, causing an increase in the number of localized states in the band gap consequently optical band gap (E_g) decreases with increasing irradiation. Furthermore, optical energy gap decreases rapidly with increasing in Hg%. It suggests that addition of Hg make more localized density of the state available. In addition, laser irradiation shows strong effect at higher Hg concentration (12%). It might be due to availability of more Hg-Se bond as Se content decreasing with increasing Hg content in the alloy. It concludes that alloy with rich Hg content is more sensitive to laser irradiation. It is also observed that absorption coefficient (α) and extinction coefficient (k) increases with laser irradiation time.

2.8 References

[1] A. Hirohata, J. S. Modera, G. P. Berera, Thin Solid Films; 510 (2006) 247.
[2] Heon Lee, Y. K. Kim, D Kim, IEEE Trans. Magn.; 41 (2005) 1034.
[3] M. S. Kamboj, G. Kaur, R. Thangaraj, Thin Solid Films; 420 (2002) 350.
[4] R K Shukla, S Swarup, A Kumar and A N Nigam, Phys stat sol (A) **1989,** 115, 105.
[5] H Yang, W Wany and S Min, J Non-cryst Solids **1986**, 80, 503.
[6] R Chiba and N Funakoshi, J Non-cryst Solids **1988**, 105, 149.
[7] K. Yilmaz, M. Parlak, C. Ercelebi, J. Mater. Sci. Mater. Electron. 2004 15 225.
[8] C. Amory, J.C. Bernede, E. Halgand, S. Marsillac, Thin Solid Films 2003 431 22
[9] E. Grison, J. Chem. Phys. 19 (1951) 1109
[10] P. Grosse, Springer Tracts Modern Phys. 48 (1969) 74.

[11] G. Weiser, J. Stuke, In: Proceedings of International Conference on the Physics of Semiconductor, vol. 1, Moscow, 1968, p. 238

[12] Adam A Bahishti, M A Majeed Khan, B S Patel, F S Al-Hazmi and M Zulfequar, J Non-Cryst Solids **2009**, 355, 2314.

[13] A V Kolo Bov, Hoyanagi and K Tanaka, J Non-cryst solids **1996**, 198-200, 709.

[14] Kojihayashi, D kato and K shimakawa, J Non-cryst solids **1996**, 198, 696.

[15] Sun Huajun, Hou Lisong, Wu Yiqun and Wei Jingsong, J Non-Cryst Solids **2008**, 354, 5563

[16] R K Pan, H Z Tao, H C Zang, T J Zhang and X J Zhao, Physica B: Condensed Matter **2009**, 404, 3397.

[17] G A M Amin, Nuclear Instruments and Methods in Physics Research Section B: Beam Interactions with Materials and Atoms **2009**, 267, 3333.

[18] R De Bastiani, A M Piro, I Crupi, M G Grimaldi and E Rimini, Nuclear Instruments and Methods in Physics Research Section B: Beam Interactions with Materials and Atoms **2008**, 266, 2511

[19] I Ivan, S Szegedi, L Daroczi, I A Szabo and S Kokenyesi, Nuclear Instruments and Methods in Physics Research Section B: Beam Interactions with Materials and Atoms **2005**, 229, 240

[20] Balboulc M R, Radiation Measurements **2008**, 43, 1360.

[21] R S Averback and M Charlie, proc of ninth International Conference on Ion Beam Modification of Materials 1996.

[22] Adam A Bahishti, M A Majeed Khan, S Kumar, M Husain and M Zulfequar, Chalcogenide Letters **2007**, 4, 155.

[23] Muneer Ahmad, J Kumar and R Thangaraj, Journal of Non-Crystalline Solids **2009**, 355, 2345.

[24] J Orava, T Kohoutek, T Wagner, Z Cerna, Mil Vlcek, L Benes, B Frumarova and M Frumar, Journal of Non-Crystalline Solids **2009**, 355, 1951.

[25] Ambika Sharma and P B Barman, Thin Solid Films **2009,** 517, 3020.

[26] A Rabhi, M Kanzari and B Rezig, Thin Solid Films **2009**, 517, 2477.

[27] M Fadel, S A Fayek, M O Abou-Helal, M M Ibrahim and A M Shakra, Journal of Alloys and Compounds, **2009**, 485, 604.

[28] Ishu Sharma, S K Tripathi and P B Barman, Applied Surface Science **2008**, 255, 2791.

[29] P Nemec and M Frumar, Thin Solid Films **2009**, 517, 3635.

[30] P R de Moura, D P Almeida and J C de Lima, Journal of Electron Spectroscopy and Related Phenomena **2007,** 155, 129.

[31] P Arun, A G Vedeshwar, Journal of Non-Crystalline Solids **1997**, 220, 63.

[32] J S Sanghera and I D Aggarwal, J Non-Cryst Solids **1999**, 256, 6.

[33] K Schwarts, The Physics of Optical Recording; Berlin, Springer-Verlag **1993**.

[34] A Pradley, Optical Storage for Computers Technology and Applications; Ellis Horwood Limited, New York **1989**.

[35] L TaiK, E Ong and R G Vadimsky, Proc Electro Chem Sc **1982**, 9, 82.

[36] A H Moharram, Thin Solid Films **2001**, 392, 34.

[37] S. Adachi, Optical Properties of Crystalline and Amorphous Semiconductors: Materials and Fundamental Principles (Springer, 1999)

[38] K. Morigaki, Physics of amorphous semiconductors (World Scientific, 1999)

[39] S. Reynolds and R. E. Belford, Physics in Technology, 18 (1987) 193
[40] M. L. Theye, Physica Scripta., T29 (1989)157
[41] J Schottmiller, M Tabak, G Lucovsky and A Ward, J Non-Cryst Solids **1970,** 4, 80.
[42] E Kh Shokr and M M Wakkad, J Mater Sci **1992**, 27, 1197.
[43] Li Zhang, Dezhi Qin, Guangrui Yang, Qiuxia Zhang Chalcogenide Letters Vol. 9, No. 3, (2012) 93 - 98
[44] M. A. Omar, Elementary Solid States Physics (Addision-Wesley, London, 1975) P.292.
[45] D. P. Machewirth, K. Wei, V. Krasteva, R. Datta, E. Snitzer, G. H. Sigel, J. Non Cryst. Solids 213-214 (1997) 295.
[46] T. Ide, M. Suzuki and M. Okada. Jpn. J. appl. Phys. 34 (1995) 529.
[47] L. Z. Mao, M. Chen and Jung Al-Lien Jpn. J. appl. Phys. 78 (1995) 2338.
[48] F. Urbach, Phys. Rev. 92 (1953) 1324.
[49] M Zanini and J Tauc, J Non-cryst solids **1977**, 23, 349.
[50] E A Davis and N F Mott, Phil Mag **1970**, 22, 903.
[51] N F Mott and E A Davis, Electronic Processes in Non-crystalline Materials 2nd edn; Oxford Univ Press **1979** p 273.
[52] Tauc J, Optical properties of Solids ed F Abeles, North-Holland **1972**
[53] Tien, C. L., and Qiu, T. Q., Heat Transfer Mechanisms during Short-Pulse Laser Heating of Metals, *Journal of Heat Transfer*, vol. 115, pp. 835–841, 1993
[54] Mao, S. S., Greif, R., Mao, X., and Russo, R. E., Plasma Development during Picosecond Laser Processing of Electronic Materials, *ASME Journal of Heat Transfer*, vol. 122, p. 424, 2000.
[55] Shirk, M. D., and Molian, P. A., A Review of Ultrashort Pulsed Laser Ablation of Materials, *Journal of Laser Applications*, vol. 10, no. 1, pp. 18–28, 1998.
[56] Asheghi, M., Touzelbaev, M. N., Goodson, K. E., Leung, Y. K., and Wong, S. S., Temperature-dependent Thermal Conductivity of Single- Crystal Silicon Layers in SOI Substrates, *Journal of Heat Transfer*, vol. 120, no. 1, pp. 30–36, 1998
[57] Kolzer, J., Oesterschulze, E., and Deboy, G., Thermal Imaging and Measurement Techniques for Electronic Materials and Devices, *Microelectronic Engineering*, Elseveir Science, vol. 31, pp. 251–270, 1996
[58] Mitra, K., Kumar, S., and Vedavarz, A., Parametric Aspects of Electron-Phonon Temperature Model for Short Pulse Laser Interactions with Thin Metallic Films, *Journal of Applied Physics*, vol. 80, no. 2, pp. 675–680, 1996.
[59] W. Kemp, "*Spectroscopy of Organic compounds*", W. H. Freeman, New York, 1991.
[60] S. K. Al-Ani, I. Al-Hassany, Z. Al-Dahan, J. Mat. Sc. 30, 3720 (1995).
[61] Hayashi Koji, D Kato and K Shimakawa, J Non-Cryst Solids **1996**, 198, 696.
[62] M Kastner, Phys Rev Letter **1972**, 28, 355.
[63] P Boolchand and P Suranyi, Phys Rev B **1973**, 7, 57.
[64] W Hoyer, B Kunsch, M Suda, and E Wieser, Z Naturforsch **1981**, 36a, 880.
[65] P Pradeep, N S Saxena and A Kumar, J Phys Chem Solids **1996**, 58, 385.
[66] S Chaudhary, S K Biswas and A Choudhary, J Non-Cryst Solids **1984**, 69, 169. [67]45
[68] S R Elliott, J Non-Cryst Solids **1986**, 81, 71.
[69] A Dahshan and K A Aly, Acta Mater **2008**, 56, 4869.
[70] O. El-Shazly, M. M. Hafiz, J. Materials Science: Materials in Electronics, **12 (7)**, (2001) 395-401

[71] Kojihayashi, D. Kato and K. Shimakawa, J. Non-Cryst. Solids **198**, 696 (1996).

[72] N. F. Mott, E. A. Davis, Electronic Processes in Non-Cryst. Mater. pp. 382 & 428 (Clarendon, Oxford, 1979)

[73] S. R. Ovshinsky and D. Adler , Contemp. Phys. **19**, 109 (1978).

[74] M. L. Theye, Proceeding of the Fifth International Conference on Amorphous and Liquid Semiconductors, Vol. **1**, 479 (1973).

[75] S. Choudhary, S. K. Biswas and A Chaudhary , J. Non-Cryst. Solids **23**, 4470 (1998).

[76] Ruby Chauhan, Ashavani Kumar, Ram Pal Chaudhary, Chalcogenide Letters Vol. 9, No. 4, (2012) 151 - 156

[77] V N Kats et al. Semicond. Sci. Technol. **27** (2012) 015009

[78] V Pamukchieva, A Szekeres and D Arsova; Phys. Scr. 83 (2011) 025405

[79] *O.I. Shpotyuk, A.O. Matkovsky, A.P. Kovalsky, M.M. Vakiv, Radiat. Eff. Defect Solids 133 (1995) 1.*

[80] *M.L. Theye, Proceedings of the Fifth International Conference on Amorphous and Liquid Semiconductors, Garmisch-Partenkichen, vol. 1, 1973, p. 479*

[81] A. Abu EL-Fadl_, A.S. Soltan, A.A. Abu-Sehly; Effect of gamma doses on the optical parameters of $Se_{76}Te_{15}Sb_9$ thin films;Journal of Physics and Chemistry of Solids 68 (2007) 1415–1421

[82] S. Chaudhuri, S.K. Biswas, Solid State Commun. 53 (1985) 273.

[83] *Zakery a, S.R. Elliott b; Optical properties and applications of chalcogenide glasses: a review ; Journal of Non-Crystalline Solids 330 (2003) 1–12*

[84] *Golovchak, R.Ya., Kozdras, A., Shpotyuk, O.I., 2008. Physical ageing in glassy As–Se induced by above-bandgap photoexposure. Solid State Commun. 145, 423–426.,*

[85] Golovchak, R.Ya., Kozdras, A., Gorecki, Cz., Shpotyuk, O.I., 2006. Gamma- irradiation-induced physical ageing in As–Se glasses. J. Non-Crys. Solids 352, 4960–4963.

[86] *Imran, M. M .A. , Al-Hamarneh, I. F. Awadallah, M. I., Al Ewaisi, M.A., 2008. Physical ageing inSe94In6 glass induced by gamma irradiation. PhysicaB403, 2639–2642*

[87] Zhao Donghui, Wang Hua, and Chen Guorongw, Gamma-Ray-Induced Multi-Effect on Properties of Chalcogenide Glasses; J. Am. Ceram. Soc., 89 [11] 3582–3584 (2006)

[88] *Amin, G.A., El-Sayed, S.M., Saad, H.M., Hafez, F.M., Abd-El-Rahman, M., 2007. The radiation effect on optical and morphological properties of Ag–As–Te thin films. Radiat. Measure 42, 400–406.*